Project Title: Assessment of HF drift data reliability

Deliverable: Final report
PI: Anna Belehaki, National Observatory of Athens (belehaki@space.noa.gr)
Date: 13 June 2005

EOARD Award FA8655-04-1-3019
Project manager: Michael Milligan

REPORT DOCUMENTATION PAGE

Form Approved OMB No. 0704-0188

1. REPORT DATE *(DD-MM-YYYY)*	2. REPORT TYPE	3. DATES COVERED *(From – To)*
30-06-2005	Final Report	23 March 2004 - 23-Mar-05

4. TITLE AND SUBTITLE

Assessment of HF Drift Data Reliability

5a. CONTRACT NUMBER
FA8655-04-1-3019

5b. GRANT NUMBER

5c. PROGRAM ELEMENT NUMBER

6. AUTHOR(S)

Dr. Anna Belehaki

5d. PROJECT NUMBER

5d. TASK NUMBER

5e. WORK UNIT NUMBER

7. PERFORMING ORGANIZATION NAME(S) AND ADDRESS(ES)

Ionospheric Group, Institute for Space Applications and Remote Sensing,
Metaxa and Vas. Pavlou str.
Palaia Penteli 15236
Greece

8. PERFORMING ORGANIZATION REPORT NUMBER

N/A

9. SPONSORING/MONITORING AGENCY NAME(S) AND ADDRESS(ES)

EOARD
PSC 802 BOX 14
FPO 09499-0014

10. SPONSOR/MONITOR'S ACRONYM(S)

11. SPONSOR/MONITOR'S REPORT NUMBER(S)
SPC 04-3019

12. DISTRIBUTION/AVAILABILITY STATEMENT

Approved for public release; distribution is unlimited.

13. SUPPLEMENTARY NOTES

14. ABSTRACT

This report results from a contract tasking Ionospheric Group, Institute for Space Applications and Remote Sensing, as follows: The Grantee will investigate use of interferometric Doppler techniques to measure drift of ionospheric particles. Determining the motion of these particles is critical in understanding their effects on HF communications and potential forecasting of atmospheric activity.

15. SUBJECT TERMS
EOARD, Space Environment, Space Weather

16. SECURITY CLASSIFICATION OF:			17. LIMITATION OF ABSTRACT	18, NUMBER OF PAGES	19a. NAME OF RESPONSIBLE PERSON
a. REPORT	b. ABSTRACT	c. THIS PAGE			MICHAEL KJ MILLIGAN, Lt Col, USAF
UNCLAS	UNCLAS	UNCLAS	UL	CD	19b. TELEPHONE NUMBER *(Include area code)* +44 (0)20 7514 4955

Table of contents

General overview of the progress reported

In the ionosphere particle drift motion involves the superposition of three main drift processes, gradient drifts, electric field drifts and drifts due to gravity. In addition to the motion imparted to the ionization due to drifts one needs to consider the effect on this motion due to the neutral atmosphere. Neutral winds and traveling ionospheric disturbances “TIDs” also cause the ionization to move. In general since the ionization is restricted to spiral along the field lines, the movement due to the interaction with the neutral atmosphere is restricted to the meridional plane. Hence the ion flow velocity parallel to the magnetic field is very complicated since many factors contribute to this velocity component, such as the neutral wind, the ion pressure gradient, the gravitational forces and TIDs. The velocity drift component in the zonal direction in comparison is simpler to interpret since it results solely due to the effect of the ambient electric field via the relationship **E = - VxB** (Scali, 1993; Kelley, 1989).

In case of HF radars such as the Digisonde, where motion is deduced from a measure of Doppler shifts on radiowaves reflected from the ionosphere a further distinction needs to be made. The Digisondes measures the Apparent Velocity “Va”, which is a complicated function of a number of time varying properties of the radio wave propagation medium. For instance the Doppler frequency shift is affected by both the motion of the reflecting surface and the time variation of the refractive index along the ray. In the ionosphere the time changes in the refractive index arise from the ionospheric motions and also from production and loss of ionization. When interpreting velocity measurements obtained from the Digisonde Drift Analysis method, care must be taken in relating the motion to the effects of photoionization, recombination, gravity waves (TIDs) and plasma motion.

It is important to setup a system that monitors ionospheric-atmospheric motions and in the same time performs quality control of the measured velocities since drift measurement technique could be valuable for scientific and operational applications.

The objective of this proposal is to assess the reliability of HF drift data, defining the conditions and limitations of using them, since the separation of different effects in data (true plasma winds or motions of phase fronts associated with plasma waves or TID caused by atmospheric gravity waves) will improve the current technique.

In the duration of the project, the following tasks have been implemented:

1. Overview of existing methodologies published in the literature concerning the analysis of HF drift measurements
2. Analysis and evaluation of the hardware and software configuration system and adjustments to optimize the Athens Digisonde performance
3. Derivation of the daily variation pattern under quiet magnetospheric conditions
4. Assessment of HF drift data reliability based on Athens Digisonde observations during days with magnetospheric substorm activity
5. Development of a web page demonstrating the real-time updated daily E and F region drift velocities plots

6. Development of a web tool for the assessment of the reliability of Athens Digisonde drift observations

Presentations in international meetings/Conferences

1. "Assessment of HF drift data reliability from Athens Digisonde", Michalareas G., A. Belehaki, I. Tsagouri, International School of Geophysics, 24th Course, Erice, Italy, September 2004.
2. "Evaluation of ionospheric drift measurements over Athens", Michalareas G, A. Belehaki, I. Tsagouri, First European Space Weather Week, ESTEC, Noordwijk, The Netherlands, 29 November – 3 December 2004.
3. "Ground based techniques and networks for monitoring the Earth's ionosphere: Latest developments in Europe", Anna Belehaki, First European Space Weather Week, ESTEC, Noordwijk, The Netherlands, 29 November – 3 December 2004 (Invited talk)
4. "Assessment of HF drift data reliability based on Athens Digisonde observations", Belehaki A., I. Tsagouri, G. Michalareas, 11th Ionospheric Effects Symposium, Alexandria, VA, USA, 3-5 May 2005 (Invited talk)

1. Overview of existing methodologies published in the literature concerning the analysis of HF drift measurements

1.1 Ionospheric Drift Processes

Three main processes are creating ionospheric drifts. The resulting effects of the three processes are usually superimposed creating the overall ionospheric drift. These three processes are: a) gradient drift, b) electric field drift, c) drift due to gravity.
The gradient drift results from the presence and the geometry of the earth's magnetic field. Two drift components are caused, one perpendicular and one parallel to the magnetic field. The perpendicular drift is caused by the interaction of the magnetic field vector and the charge of ions or electrons. The parallel drift component results due to the curvature of the magnetic field lines. Because of this curvature the particles, which follow the perpendicular drift around the magnetic field vector, also experience a centrifugal force due to the curvature of the magnetic field lines.

$$Ugd = \frac{\varepsilon_{\perp} + 2\varepsilon_{\parallel}}{qB^3}\left(\underline{B} \times \nabla_{\perp} \mid \underline{B} \mid\right) \qquad (1)$$

where

$\varepsilon_{\perp}$: Particle kinetic energy $\perp$ to magnetic field direction
$\varepsilon_{\parallel}$: Particle kinetic energy || to magnetic field direction
q : Particle charge
B : Magnetic Field

The electric field drift results from the presence of an electric field. This motion is in the direction perpendicular to both the magnetic and the electric fields. The combined effect of these two motions is a spiraling drift on the plane defined by the magnetic and electric fields and with direction perpendicular to them. The direction of spiraling drift depends on the charge of the particle while the direction of the translational drift is independent of it.

$$Ued = \frac{1}{B^2}\left(\underline{E} \times \underline{B}\right) \qquad (2)$$

where E: Electric Field

The drift due to the force of gravity is in the direction perpendicular to the magnetic and gravitational fields when no electric field is present. The spiraling motion is again driven by the direction of the geomagnetic field.

$$Ued = \frac{q}{mB^2}\left(\underline{g} \times \underline{B}\right) \qquad (3)$$

where

m : mass of ion species
g : Vector gravitational acceleration

Apart from the above-described processes, which cause drifting of plasma due to the effect of magnetic, electric and gravitational fields, other processes such as neutral winds and travelling ionospheric disturbances (TID's) can also cause movement of ionospheric plasma. Because the charged particles are restricted to spiral along the field lines, the resulting drift effects of phenomena not involving electromagnetic or strong gravitational forces are restricted to the meridional plane. Due to this fact the drift velocity components parallel to the magnetic field of the earth contains the effect of a large number of factors, such as gravity gradients, neutral winds, ion pressure gradients and travelling ionospheric disturbances. The drift velocity component in the zonal plane is simpler to be analyzed.

1.2 Drift measurements using specular reflection of HF signals

Ionosondes operate like High Frequency Doppler radar systems measuring echo amplitude and phase, angle of arrival, polarization and Doppler spectrum as a function of range (Reinisch et al., 1998). Pfister (1971) was the first to suggest the use of HF phase measurements and spectral analysis in ionospheric sounding. The mode of the ionosonde, which is responsible for the estimation of the ionospheric drift measurements, is the interferometric Doppler technique. The main methodology for measuring ionospheric drifts using specular reflection, involves the signal transmission by the transmitter antenna and its reception, after its reflection in the ionosphere, by 4 or more receiver antennas located appropriately, about one wavelength apart, in a triangle configuration. By altering the frequency of the transmitted signal, the reflection is achieved in different layers of the ionosphere, allowing thus to identify drifts in various heights. The drift velocity that can be identified by this method is the velocity of the motion of the ionized particles in the ionosphere at various heights. This velocity incorporates the effect of all the processes that can cause drifting. "In contrast to incoherent or coherent scatter radar systems which observe backscattered radio energy, ionosonde sounding is based on total (specular) reflection which occurs at the level where the wave frequency f is equal to the plasma frequency fp (for the ordinary polarization)" (Reinisch et al., 1998).
The driving variable of this method is the observed Doppler shift amplitude and phase of the received signal at each of the receiving antennas. Actually, this Doppler shift is not entirely caused by the movement of the reflecting ionospheric layer. Other processes such as the variation of the intermediate refractive index values during the propagation of the signal, contribute also to this shift. The phase path P of a ray between points A and B is given by:

$$P = \int_{A}^{B} \mu \cos \alpha ds \qquad (4)$$

where

μ: refractive index at a point on the ay path
α: angle between the wave normal and the ray direction

The integration is carried out along the ray path. Now if the ray is travelling along a time varying medium and is reflected on a moving surface, then according to ray theory (Bennett, 1968) the time derivative of the phase path is given by the general expression:

$$\frac{dP}{dt} = \int_A^B \frac{\partial \mu}{\partial t} \cos a ds + \left[p \cdot v \right]_A^B \tag{5}$$

where

p : vector in the direction of the wave normal with magnitude μ
v : vector velocity of a point on the array

The Doppler shift is defined as:

$$\Delta f = -\frac{f}{c}\frac{dP}{dt} \tag{6}$$

where

f : frequency of radio wave
c : speed of light
P : Phase path

In usual practice dP/dt is referred to the contribution due to the ray travelling from the transmitter to the point of reflection. The actual value obtained experimentally will be of course twice this amount.

a) Reflector in free space

If it is assumed that the reflector is travelling in free space then (5) becomes:

$$\frac{dP}{dt} = \hat{p} \cdot v_R \tag{7}$$

where

$\hat{p}$: unite vector in the direction of the ray path
v_R : velocity of the point of reflection with respect to the observer

If we assume a situation like the one pictured in figure 1 where the reflector is moving as a whole with a velocity u and the point of reflection is moving along the reflection surface with velocity w, then:

$$v_R = u + w \tag{8}$$

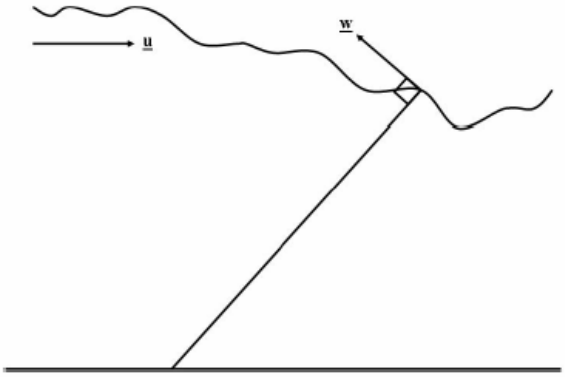

Figure 1: Ray geometry for a reflector moving with velocity u in free space. w is the velocity of the reflecting point along the reflector surface.

Noting that w is perpendicular to $\hat{p}$, equation (7) becomes:

$$\frac{dP}{dt} = \hat{p} \cdot u \tag{9}$$

The above expression simply states that dP/dt equals the magnitude of the velocity component along the line of sight. In the simplest of cases where the reflecting surface is assumed to be moving horizontally with a speed u_H, equation (9) becomes:

$$\frac{dP}{dt} = u_H \sin\theta \tag{10}$$

where

θ : angle of arrival measured from the zenith

Thus in this case the speed can be determined by measuring the time rate of change of the phase path and the angle of arrival.

b) Medium of constant refractive index

If in the same situation as the one in figure 1, the reflector is moving through a medium of constant refractive index μ then equation (5) becomes:

$$\frac{dP}{dt} = \mu \hat{p} \cdot u \tag{11}$$

Again in the simplest of cases where the reflecting surface moves horizontally with velocity u_H we have:

$$\frac{dP}{dt} = \mu u_{\mathrm{H}} \sin\theta \tag{12}$$

In this case, in order to determine the velocity also the refractive index μ must be known.

c) Medium with spatially varying refractive index

The time derivative of the phase path is the integral of the entire path divided in small segments, each one multiplied by the corresponding rate of change of the intermediate refractive index plus the path created due to the reflection of the wave on a drifting surface multiplied by the refractive index at the point of reflection. The expression for the time derivative of the phase path is (Scali, 1993):

$$\frac{dP}{dt} = \int_0^r \frac{\partial \mu}{\partial t} \cos a ds + \mu_r \hat{p}_r \cdot u \qquad (13)$$

where

μ : refractive index
μ_r : refractive index at the reflection point
$\hat{p}_r$: Unit vector in the wave normal direction at the reflection point
a : angle between wave normal and the ray direction
u : speed of the reflection point

In this situation both the motion of the reflection point and the time variation of refractive index along the ray path contribute to dP/dt. For the ionosphere, time changes of refractive index may arise from ionospheric motions or from production and loss of ionization.
If the rate of change of the refractive index of the medium is symbolized by a constant velocity v with respect to the observer then the problem is simplified by considering a frame of reference moving with the medium. In such a frame of reference there are no time changes in refractive index along the ray path but both end points of the ray are moving. The observer is moving with velocity $-v$ and the reflection point is moving with velocity $(u-v)$. This situation is described in figure 2. In this situation equation (5) becomes:

$$\frac{dP}{dt} = \mu_o \hat{p}_o \cdot v + \mu_r \hat{p}_r \cdot (u - v) \qquad (14)$$

where

μ_o : refractive index at the observer
$\hat{p}_o$: Unit vector in the wave normal direction at the observer

In the most common methodologies of ionospheric measurements, reflection occurs at $\mu = 0$ and this presents a special difficulty because the ray theory assumptions break down at this point (Bennett, 1968). However as the reflection point approaches the level at which $\mu = 0$, the contribution to dP/dt due to the motion of the reflection point (i.e. $\mu_r \hat{p}_r (u-v)$) approaches zero. Hence dP/dt is due almost entirely to the relative motion of the whole medium with respect to the observer rather than the reflection point per sec (Dyson, 1975).

For experiments performed from the ground is $\mu_0 = 1$, so that in the observer's reference frame, equation (9) becomes:

$$\frac{dP}{dt} = \hat{p}_o \cdot v \tag{15}$$

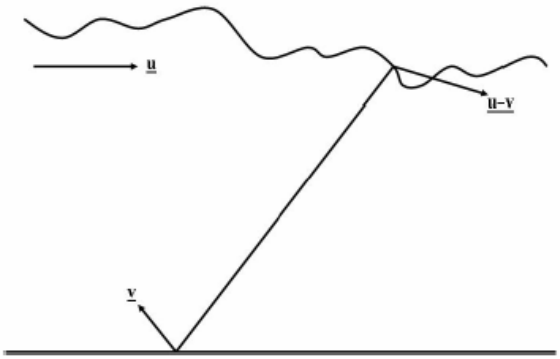

Figure 2: Ray geometry for a reflector moving with velocity u in a horizontally stratified medium which is itself moving with velocity v with respect to an observer.

The above result is valid for the case that the medium moves with a uniform velocity. If the velocity of the medium is not uniform then the results are quite different. In this case the refractive index can be represented as $\mu(x, y, z)$ where x, y, z are functions of t and equation (13) becomes:

$$\frac{dP}{dt} = \int_0^r \left(u_x \frac{\partial \mu}{\partial x} + u_y \frac{\partial \mu}{\partial y} + u_z \frac{\partial \mu}{\partial z} \right) \partial t \cos a ds + \mu_r \hat{p}_r \cdot u \tag{16}$$

where the velocity of the medium is:

$$v = u_x i + u_y j + u_z k \tag{17}$$

In this case the velocity cannot be determined only by measurement of dP/dt and the angle of arrival as in all the other cases. Thus if measurements are only made on one frequency the interpretation is uncertain. However if measurements are made on two frequencies (or ordinary and extraordinary components of one frequency) the same velocities will be deduced from each set of measurements if time changes in refractive index arise only from bulk motions of the medium (Dyson, 1975).

The time changes in the refractive index arise from ionospheric motions and also from production and loss of ionization. When interpreting velocity measurements obtained from the Digisonde Analysis method, care must be taken in relating the motion to the effects of photoionization, recombination, gravity waves (TID's) and plasma motion. During those periods when only the movement of the ionization is responsible for the movement of the reflecting

medium then $V = V_a$ and the Digisonde drift velocity measurement represents the motion of charged particles in the ionosphere (Scali, 1993).
To decompose the signal into its Doppler components the ionosonde performs a Fast Fourier transform for each antenna signal.

1.3 Determination of drift velocities

The following basic methodologies have been analyzed:

1.3.1 Determination of drift velocities by evaluating the echo-location and the velocity for each echo

The determination of ionospheric drift velocities incorporates two steps. First the evaluation of the echo location and then the evaluation of the velocity for each echo. The location of each echo is described by the arrival angles of elevation θ and azimuth ϕ. This formulation was adopted in the method devised by Scali et al. (1995) to be applied in the Digisonde. The mathematical description of this methodology for the evaluation of the echoes' angles of arrival is the following:

The phase difference between two antennas j and i in the multi-antenna configuration is evaluated by:

$$\Delta\phi_{ji} = \phi_j - \phi_i = \bar{k} \cdot \left[\bar{r}_j - \bar{r}_i\right] \tag{18}$$

where

$\bar{k}$: Vector wave number
$\bar{r}$: Position vector of antenna

As the vector wave number $\bar{k}$ describing the direction of reflection consists of three coordinate components $\left[k_x, k_y, k_z\right]$ three equations are enough to determine these three components.
In the least squares formulation of this determination all the possible antenna combinations can be used and this means that more than 3 equations can be used for the evaluation of the 3 coordinate components of $\bar{k}$. In order to derive the optimal solutions for $\bar{k}$ the derivatives of least squares with respect to k_x, k_y, k_z must be equal to 0.

Then $k = \begin{bmatrix} k_x \\ k_y \\ k_z \end{bmatrix}$ can be determined by:

$$K = -A^{-1}\Phi \tag{19}$$

where A and Φ are matrices containing parameters arising from the mathematical manipulation of the three partial derivatives, which can be calculated since they contain the coordinates of the individual antennas (Δx_{ji}, Δy_{ji}, Δz_{ji}) and the phase difference $\Delta\varphi_{ji}$ between the three antennas.

The coordinates of the individual antennas are a priori known and the Digisonde measures the phases. So the vector wave number coordinate components can be calculated from equation (19). From the coordinate components of $\bar{k}$, the azimuth and elevation angles ϕ, θ and the corresponding unit position vector R can be evaluated for each reflectors. Then the velocity coordinate components can be evaluated by least squares fitting to 3 or more reflectors' data. Considering that if the ionosphere is moving with velocity $\bar{u}_D$, then each echo s will have its characteristic Doppler shift d_s.

This is the general theory of determining ionospheric drift velocities by methods based on specular reflection of HF signals. The method applies when data from 3 or more echoes is used. These 3 or more sources must be moving with the same velocity in order the resulting drift to be physically meaningful. In the case that the entire ionosphere in the field of view of the sounder is moving with a uniform velocity then any combination of 3 or more sources should give similar velocity results. In this case all the echoes found by equation (19) can be used in the least squares fitting procedure in order to evaluate a single common drift velocity vectors for the entire overhead ionosphere. This technique has been applied in the Digisondes Drift Analysis since their development (Reinisch, 1987; Cannon et al., 1991; Smith, 1998). Thus the Digisonde software provides one velocity vector value for each measurement, although a large number of echoes are involved. Additionally it provides the standard deviation of the error resulting from the least squares fitting procedure.

Scali et al. (1995) performed a comparative study of drifts evaluated by the above techniques and the more accurate Incoherent Scatter Radar Technique at Sondrestromfjord. He found that although the average velocity was in good agreement, there were significant errors, which were attributed to three main reasons:

- The velocity is not uniform within the field of view.
- The velocity is not stationary during the measurement.
- Spectral aliasing in the Fourier transform.

For this reason the use of the data from all the echoes in a measurement for the derivation of a single velocity vector was questioned. To create a more realistic representation of the ionospheric drifting profile a new method was devised. The Generalized Digisonde Drift Analysis(GDDA) evaluates several velocities using the many simultaneous sources. This method is providing a great advantage of drift measurements by Digisondes against Incoherent Scatter Radar methods because the latter can only resolve different velocities by steering the dish in more than three different directions and assessing the observed line-of-sight velocities. These measurements are done sequentially and therefore require a longer time, which may cause problems in the presence of time varying velocities (Reinisch, 1998). The GDDA method uses all the possible combinations of the observed echo sources in triplets and evaluates the velocity vector for each triplet. Then the resulting distribution of all the velocities is examined. All the combinations for which the three sources move with the same velocity show a peak in the distribution. By this way the GDDA method locates different velocities at different locations of the overhead ionosphere.

1.3.2 Determination of the two angles of arrival

Pfister (1974) developed a methodology of determining the two angles of arrival. The two angles of arrival are defined both on the azimuthal plane defined by the magnetic north-south and east-west axes. They are defined as:

φ : angle of arrival from the North-South axis
θ : angle of arrival from the East-West axis

These two angles are not evaluated from the vector wave number but each one is evaluated separately, directly from the phase and Doppler shift measurements The antenna system used for this method is identical to the system already presented in figure 3.

Let us denote the Doppler shift by Ω. Then according to Pfister (1971):

$$\frac{\Delta\phi_{ji}}{\Delta\Omega_{ji}} = \frac{|r_{ji}|\cos\theta_{ji}}{2V} = \Delta t_{ji} \qquad (20)$$

The angle θ_{ij} is the angle between the velocity vector and the axis coinciding with the vector $\bar{r}_{ji}$ where j, i are the antennas used in the pair.

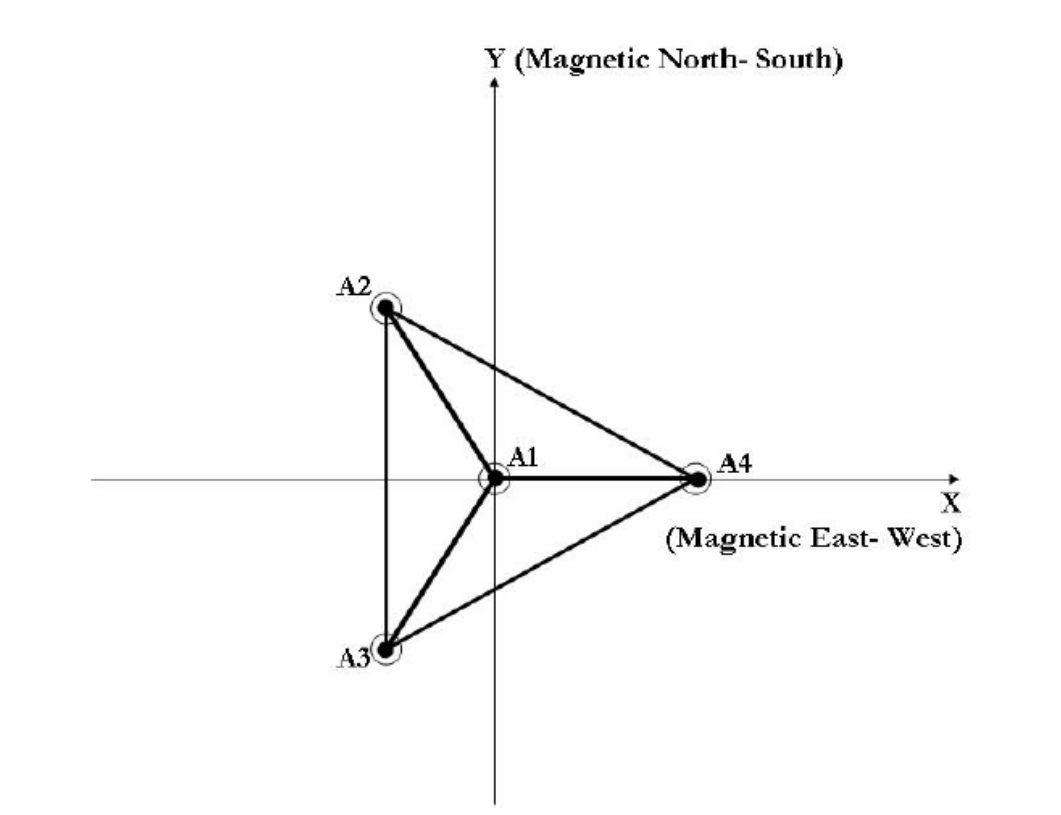

Figure 3: Ideal 4 antennas configuration relative to magnetic north

If the movement of the ionosphere is a plane wave motion then the resulting angles should be complementary. Deviation from this norm reveals that non-plane wave characteristics exist in the motion of the ionosphere.

1.3.3 Methodology for distinguishing between different types of disturbances

Wilson (1995) developed a methodology for distinguishing between the following types of disturbances namely:

- Non-dispersive plane wave motions.
- Non-plane wave motions, which obey Pfister's theorem.
- Dispersion, where the spectral components of a single disturbance travel with different speeds but in the same direction.
- Superposition, where the effects of disturbances produced by more than one source are being observed simultaneously.

Wislon follows the same methodology as Pfister (1974) and Bronwlie et al. (1973) in the definition of angle of arrival, which is different than the one followed by Reinisch et al. (1998). In this interpretation the drifting motion is examined in each axis separately. Figure 4 shows the pattern of vertical reflection from a plane surface moving in parallel to axis X and figure 5 shows the pattern of vertical reflection from an undulated surface moving also in parallel to axis X. In the later case the lines of constant ray path corresponding to the case of vertical reflection from a plane surface are shown with their new directions due to the reflection from the undulated surface. As it seen from figure 5, over a large portion along the ground an interference of three rays is observed. If we assume the undulated moving surface as a plane wave propagating in the x direction then the zenith angle is given by:

$$\sin\delta = \frac{ds}{dx} \tag{21}$$

where s is the distance from the ground along the ray direction to the plotted and point of the particular ray. The phase of the reflected signal is given by

$$\phi = \left(\frac{2\pi}{\lambda}\right) 2\left(S + s\right) \tag{22}$$

where λ is the wavelength of the operating frequency and S is the fixed length of the ray as plotted in figure 4. The factor 2 takes care of the round trip of the signal. According to simple geometry and with the assumption that only one horizontal velocity exists in parallel axis X, the Doppler shift in frequency for individual rays (n) becomes:

$$\Omega_n = \frac{d\phi_n}{dt} = \frac{4\pi}{\lambda} u \sin\delta_n \tag{23}$$

This relationship can be extended to three dimensions as:

$$\Omega_n = \frac{d\phi_n}{dt} = \frac{4\pi}{\lambda} u_x \sin \delta x_n + \frac{4\pi}{\lambda} u_y \sin \delta y_n + \frac{4\pi}{\lambda} u_z \sin \delta z_n \qquad (24)$$

Where:

$\phi = \delta y_n$, the zenith angle measured on the y-z plane from the motion along the y (Magnetic North-South) axis.
$\theta = \delta x_n$, the zenith angle measured on the x-z plane from the motion along the x (Magnetic East-West) axis.

(25)

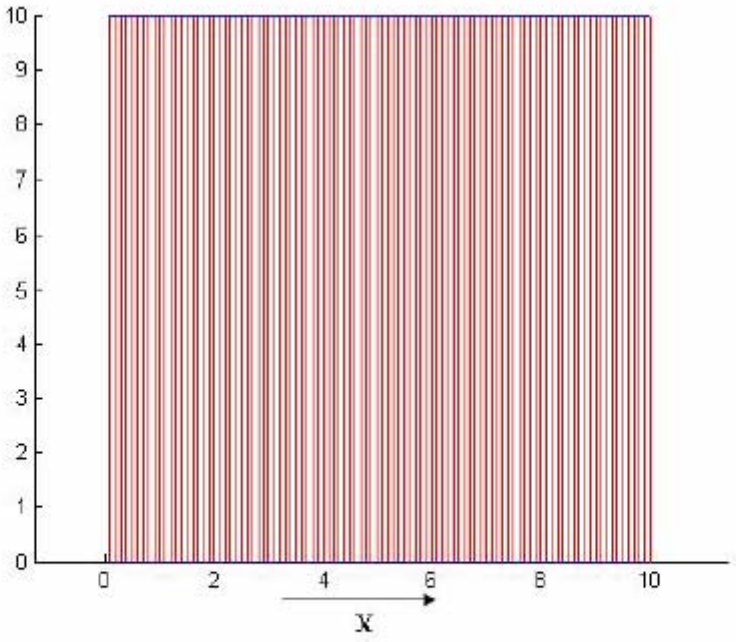

Figure 4: Pattern of vertical reflection from plane surface

Equation (30) can be expressed in terms of the rate of change of the phase path as:

$$\frac{dR_n}{dt} = u_x \sin \theta_n + u_y \sin \phi_n + u_z \qquad (26)$$

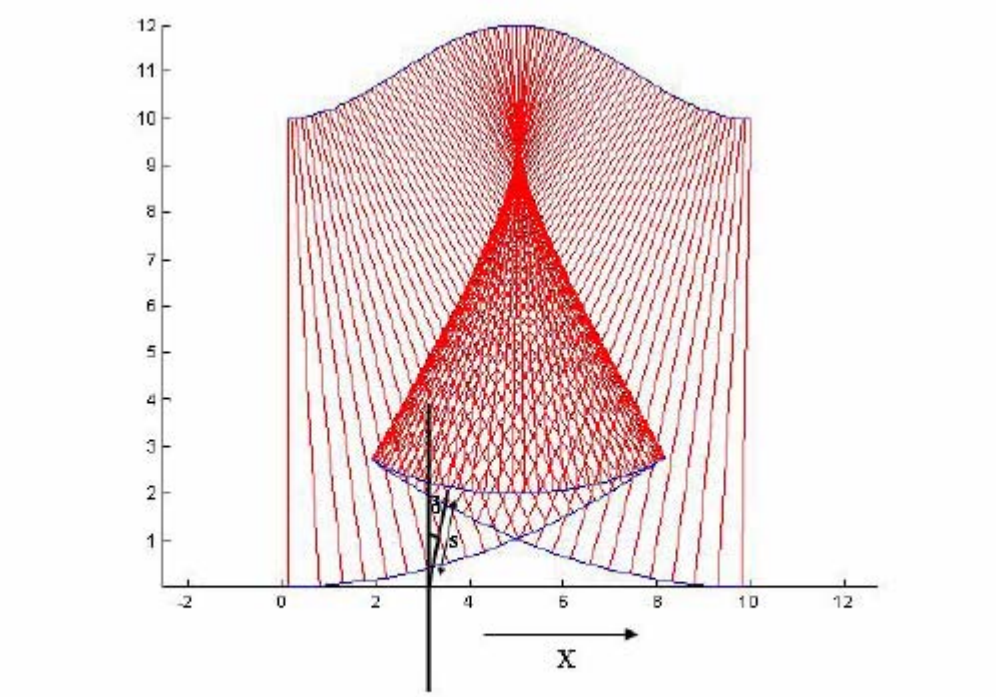

Figure 5: Pattern of vertical reflection from undulated surface

This relationship is valid for any two-dimensionally defined reflection surface moving as a whole perpendicular to the third direction (Pfister, 1971). This relationship has been called *Pfister's theorem*. The angles θ and ϕ from eq. (25) are named East-West and North-South angles of arrival. It is important to mention that they are both zenith angles measured in 2 different planes, each one defined by the z axis and the corresponding second axis. The evaluation of these two angles is a straightforward process that makes the assumption that two perpendicular movements are observed, one parallel to the x axis and one parallel to the y axis. The phase difference of the antenna pair 1-4 is used to evaluate the East-West zenith angle and the phase difference on the antenna pair 2-3 is used to evaluate the North-South zenith angle. Because it is assumed that the two motions are in parallel to the two axis x, y, equation (18) is simplified and the for the two pairs the following equations are assumed true:

$$\Delta\phi_{32} = \phi_3 - \phi_2 = k_y \cdot (y_3 - y_2) \tag{27}$$

$$\Delta\phi_{41} = \phi_4 - \phi_1 = k_x \cdot (x_4 - x_1) \tag{28}$$

From the above equations k_x and k_y, the wave numbers for the two perpendicular motions are evaluated. The wave numbers are then related to the direction of motion as:

$$k_y = \frac{2\pi}{\lambda} \sin\theta \cos 0^o \tag{29}$$

$$k_x = \frac{2\pi}{\lambda}\sin\phi\cos 0^o \tag{30}$$

The term $\cos 0^o$ is included above in order to show the basic assumption that the two motions are parallel to the x and y axes respectively. From equations (29, 30) the two zenith angles can be evaluated. According to Wilson (1995) if the movement of the ionosphere follows a plane wave motion then there should be a linear relationship between the two zenith angles, resulting from all the echoes received during a single measurement. This comes from the fact that if the velocity is towards a single direction as in the case of plane wave motion then the rate of the coordinate components of this velocity along the x and y-axis should be constant. This means that the rate of the sinus of the zenith angles should remain constant. The sine of multiple angles can be written as:

$$\sin(nx) = \sum_{k=0}^{n} \cos x^k \sin x^{n-k} \sin\left[\frac{1}{2}(n-k)\pi\right] \tag{31}$$

If we neglect all the terms that have powers of sine greater than 1 and we also assume that the zenith angles are close to 0^o (measured from z axis), which gives also the assumption $\cos(nx) \cong 1$ we take the approximate relation:

$$\sin(nx) = n\sin x \tag{32}$$

So if the rate of the sinus of the zenith angles should remain constant then the rate of the zenith angles themselves should remain constant as well. Wilson (1995) used this fact in order to establish his first test of distinction between different types of ionospheric movements. He fitted a linear function to the measured zenith angles and examined statistically the resulting error. If the error was small then indeed the relationship between the zenith angles was linear in reality and this meant that a plane wave motion was identified. If the relationship was not linear then the motion was not a plane wave.

After the examination of the relationship between the angles of arrival, Wilson (1995) evaluated the velocities by least squares fitting of *Pfister's Law* to measurements. Then by statistical interpretation of the resulting error he examination if the overhead moving ionosphere obeyed *Pfister's Law*. Small error showed that the movement obeyed the law and large error the contrary. The types of movements, which were identified by these two consequent tests, are summarized in Table 1 (Wilson, 1995).

Motion Description	φ vs θ	dR/dt vs θ	dR/dt vs φ	Pfister's theorem obeyed
Non-dispersive plane wave	L	L	L	Yes
Dispersive	L	N/N/L	N/L/N	No
Superposed	N	N	N	No
Non-plane wave obeying Pfister's theorem	N	N	N	Yes

L : Linear, N : Non-linear

Table 1: Types of motions distinguished by the relationships between the rate of the phase path and the angles of arrival.

1.3.4 Velocity determination of different concurrent waves in the ionosphere

Bronwlie et al. (1973) derived a methodology based on Fourier analysis in order to derive the velocities of various concurrent waves, which superimposed cause the observed movement of the ionosphere. The basic variables, which are needed in order to derive the velocities, are the angle of arrival θ and the rate of the phase path dR/dt as defined in equation (26). Brownlie et al. (1973) examined only the motion parallel to the x axis and thus only the angle θ is used in their analysis. So the relationship between the angle of arrival and the rate of the phase path is defined as:

$$\frac{dR}{dt} = u \sin\theta \tag{33}$$

If there are several reflections, for each reflection we would measure θ and dR/dt and should obtain the same velocity if there is no dispersion. If $\sin\theta$ and dR/dt do not show a linear relationship, the reflecting structure must be changing in form as it moves, or in other words, dispersion is present. Bronwlie at al. (1973) supposed in this case that this kind of structure consists of a number of sinusoidal waves having various velocities.
If z is the height of the reflector then:

$$\left[\frac{dz}{dt}\right]_n = -V_n\left[\frac{dz}{dx}\right]_n \approx \left[\frac{dR}{dt}\right]_n \tag{34}$$

As dz/dt at a given value of x may be expressed:

$$\frac{dz}{dt} = \sum_n \left[\frac{dz}{dt}\right]_n \tag{35}$$

it may also be written that:

$$\frac{dR}{dt} = \sum_n \left[\frac{dR}{dt}\right]_n = \sum_n V_n\theta_n \tag{36}$$

where θ_n is the slope of the reflector.

A conventional Fourier analysis may be performed on the measured values of dR/dt and θ with time in order to separate the components $(dR/dt)_n$ and θ_n on the assumption that $R\sin\theta$ is sufficiently small. The velocity of the nth component is then found by:

$$V_n = \frac{\left[\frac{dR}{dt}\right]_n}{\theta_n} \tag{37}$$

The relative phases of $(dR/dt)_n$ and θ_n should be zero or π. If there is no correlation between peaks of dR/dt and θ as functions of ω, then (63) would not give reliable velocities. Noise in the data or the presence of vertical velocities would reduce correlations, any peak in the $(dR/dt)_n$ spectrum not corresponding to one in θ_n spectrum could be due to a vertical velocity or the presence of standing waves. Bronwlie et al. (1973) developed such a method, which was tested successfully with model data but did not guarantee convergence. From et al. (1988) developed an improved iterative method based on least squares fit to data which always converges. This method uses the same harmonic expression for the derivation of the height of the reflector.
According to this method the angle φ and the rate of change of the range dR/dt are given by:

$$\phi = \sum i(k_{nx} + il_{nx})A_n \exp i\left(\omega_n t - k_{nx}R\phi - k_{ny}R\theta\right)\left(1 + l_{nx}R\phi + l_{ny}R\theta\right) \qquad (38)$$

$$\frac{dR}{dt} = \sum i\omega_n A_n \exp i\left(\omega_n t - k_{nx}R\phi - k_{ny}R\theta\right)\left(1 + l_{nx}R\phi + l_{ny}R\theta\right) \qquad (39)$$

where the wave number k has real components k_x and k_y and imaginary l_x and l_y in the x and y directions. A_n is the amplitude, ω_n the angular frequency and k_n the wave number of the n^{th} wave. The above equations can be used to identify the amplitude and wave number of each of the harmonic components contribution to the overall wave motion of the ionosphere. The validity of the above method is questioned for specific cases such as the case of a single cloud of ionization (sporadic E-s example). However, whenever z has a single value for all x, y and t around the radar the data must be consistent with the dispersion model. For the treatment of such cases From et al. (1988) developed a geometric method of constructing from measurements an effective equivalent surface of reflection which exists for at all x, y and t.

1.3.5 Resolution of angle of arrival

Whitehead and Monro (1975) derived a general expression for the resolution of the angle of arrival. By assuming that an echo is reflected back to the transmitter at the off-vertical angle θ, the Doppler shift f is given by:

$$f = \frac{-2V\theta}{c} f_0 = \frac{-2V\theta}{\lambda} \qquad (40)$$

provided $\theta << 1$. Here c is the velocity of light, f_0 the transmitted frequency and λ the radio wavelength in free space. This is a simplified form of Pfister's equation (26) and takes account of the reflector's motion relative to the reflector. The Doppler shift does not stay constant with time because θ changes. As Whitehead and Monro (1975) state, the rate of change of θ depends on the curvature at the reflection point and thus they use only a simple approximation to the rate of change of θ. This is:

$$\frac{d\theta}{dt} \approx \frac{V}{H} \qquad (41)$$

where H is the height of the reflector. From (40) and (41) the rate of change of the Doppler shift can be calculated by:

$$\frac{df}{dt} \approx \frac{-2V^2}{cH} f_0 \tag{42}$$

As the Doppler spectrum is derived by the Fast Fourier Transform, the maximum useful time of observation T may be defined so that the frequency resolution $f\left(\approx \frac{1}{T}\right)$ between the Fourier components is equal to the change in Doppler shift of any echo in the time T. That is:

$$\Delta f = \frac{1}{T} = \frac{2V^2}{cH} f_0 T \tag{43}$$

and consequently

$$\Delta f = \frac{1}{T^2} = \frac{2V^2}{cH} f_0 \tag{44}$$

By using (40) and (44) the angular resolution can be calculated as:

$$\Delta\theta = \frac{c\Delta f}{2Vf_0} = \sqrt{\frac{\lambda}{2H}} \tag{45}$$

This means that echoes coming from reflection points only a Fresnel zone apart may be resolved using Fourier analysis.

2. The Athens HF radar: hardware and software configuration

A state of the art infrastructure to monitor the Earth's Ionosphere is operating in the National Observatory of Athens since September 2000. The ionospheric station is a Digital Portable Sounder with four receiving antennas, spaced about one wavelength apart. The various separation distances of the receivers are repeated in six different azimuthal planes. This six-way symmetry is exploited by defining the six azimuthal beam directions along the six axes of symmetry of the array, making the beamforming computations very efficient. The station can operate in four different modes: 1) Scanning ionogram, 2) Drift ionogram 3) Fixed Frequency ionogram 4) Oblique ionogram.

Real-time ionograms with the results of their automatic scaling and the history of past soundings are currently available on the official web site of Athens Digisonde (http://www.iono.noa.gr).

For the post-processing of the drift ionogram, the Digisonde Drift Analysis (DDA) tool is installed in Athens Digisonde for automatically measure F-region plasma drifts by detecting the Doppler shift and angle-of-arrival of echoes. Each resulted sky map generally contains a large number of sources. Any three separated sources within a skymap with their los velocities give the plasma velocity, as long as all three move with the same velocity. Since it is not known a priori which sources move with the same velocity it is necessary to try all combinations of three sources and inspect the resulting velocity distribution. All combinations for which the three points move with the same velocity will produce the same or similar velocity values depending on the signal-to-noise ratio, and the number of occurrences of this value will show a peak (Reinisch et al., 1998).

The types of data selected originally from Athens Digisonde (until June 2004) according to the default setup are:

1. Doppler ionograms in RSF format which allows for two bytes for each sampled height to store a multi-beam directional measurement. O and X data are stored in separate arrays.
2. Raw Drift data for input to the DDA program. The complex amplitude Doppler spectra are stored separately for all heights requested and for each antenna, in order to detect angles of arrival for each Doppler component.
3. Sky maps showing the locations of the radio sources (reflection points) each source having its own line-of-site (LOS) velocity. The velocity vector of the moving plasma is obtained from the set of LOS velocities.
4. Drift velocities calculated with the DDA method corresponding to the peak of a distribution of velocities
5. Daily Directograms giving the direction of the recorded echoes versus their height.

The raw data is restricted to the Drift options chosen by the Digisonde operator, i.e. frequency, height and polarization gates are set. Hence it is up to the operator at the station to set modes which will optimize the type of observation that is required, for a specific campaign, or for routine monitoring of the ionosphere. On running a drift program, vertically transmitted HF radio waves illuminate a large area of several hundred kilometers in the F-region. An array of crossed loop antennas receives the signals reflected back from the ionosphere and separate these signals

into O and X-polarizations. The time series received at each antenna is Fourier transformed in real time resulting in four complex spectra being recorded in the Drift file. At this time a quality control of the digisonde system and data is done. The echo location plots of the reflected signals are simultaneously calculated producing the Skymap data set. Once the source positions are located and their Doppler shift recorded the Va velocity components are calculated.

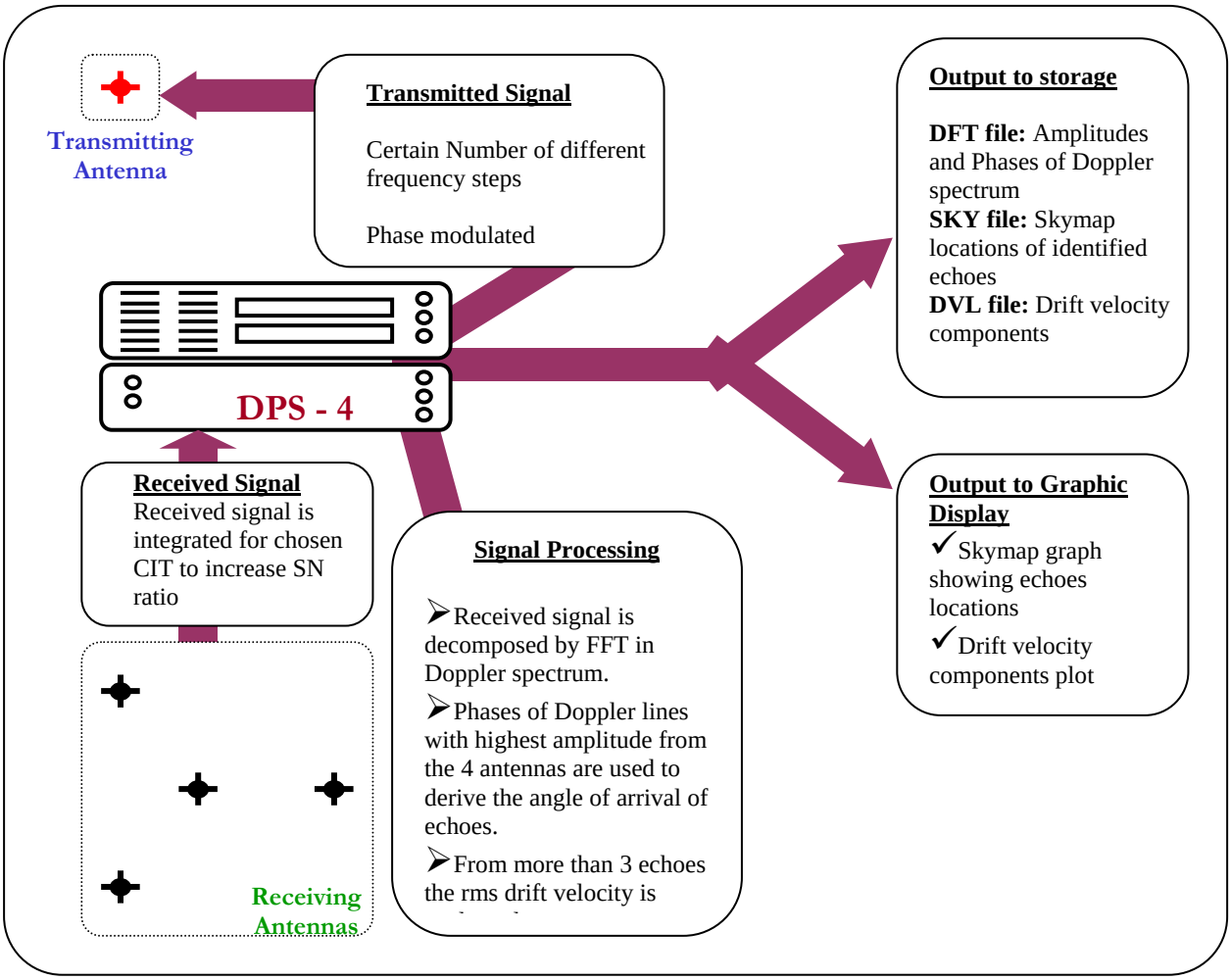

Fig.6: Schematic representation for the signal reception and processing and the data storage and display.

The DDA software is configured in each station taking into account its local characteristics and the geometry of the receiving antennas array. The ideal layout of the receive antenna array consists of four antenna stations, three of which form an equilateral triangle, the fourth station is located at its centriod (Figure 7). Each receive antenna station comprises four crossed-loop active measurements.

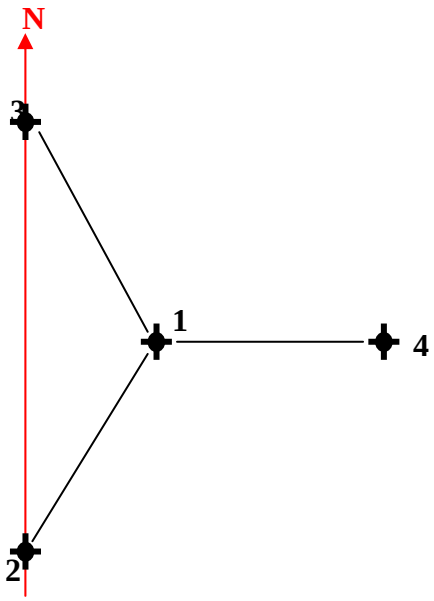

Figure 7: The ideal layout of the receive antenna array.

In the case of Athens Digisonde the configuration is not ideal and the actual geometry appears in Figure 8. The actual coordinates of the receiving antennas in the compass magnetic coordinate system are given in Table 2. The DDA software parameters were adjusted according to the actual configuration of the receiving array installed in Athens site.

Table 2: The coordinates of the Athens Digisonde receiving array

	Ant 1	Ant 2	Ant 3	Ant 4
X	0.000	36.0700	-24.3300	-20.7400
Y	0.000	13.4500	13.4500	35.8200

The control program was also configured in order to modify the sounding parameters. Since the height resolution of drift measurements is an important consideration (Parkinson and Dyson, 1998), the height resolution was set equal to 5 km (that corresponds to 33.3 μs for the half-power full width of the available transmitter pulses), and the data collection was at 5 km steps in range. In the drift mode the DPS-4 is limited to the data collection at a predetermined combination of four frequency-range bins (FRBs). One hundred twenty eight quadrature samples are recorded (Number of Integrated Repetitions equal to 7) on the total sum of four receiving antennas using o-polarisation at a pulse repetition rate of 50 Hz and complementary phase codes (533 μs pulse). The duration of each concurrent time series is given by 128 (Doppler resolution) x 2 (code order) x 1 (polarisation) x 4 (FRBs) x 1/50 (pulse rate) = 20.48 s. Hence the spectral resolution was 0.049 Hz.

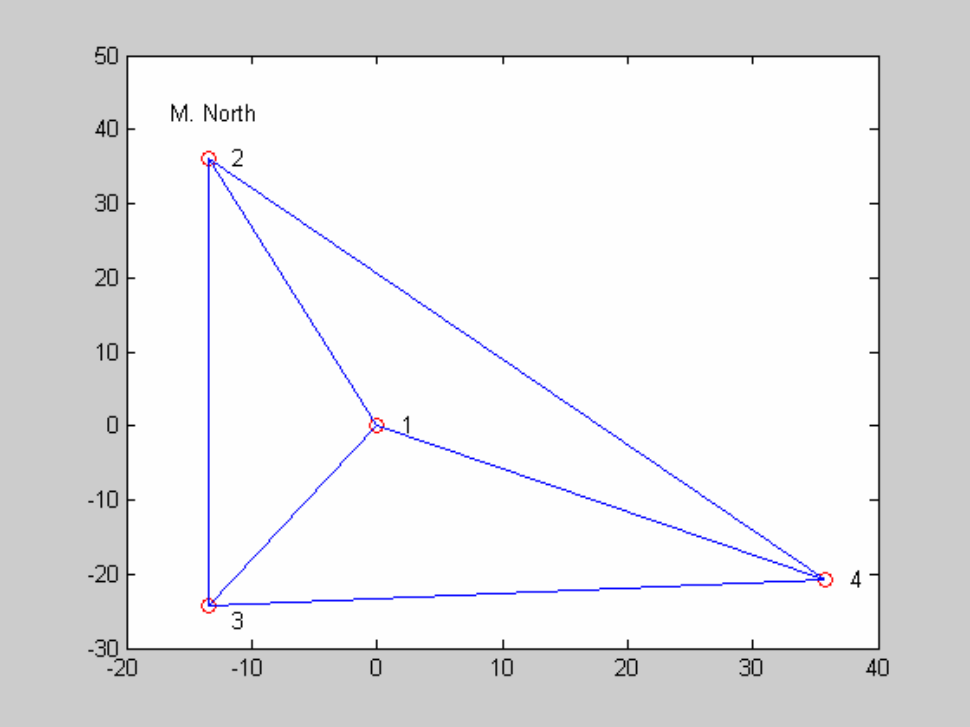

Figure 8: The geometry of the Athens Digisonde receiving array

Then, the configuration file that controls the behaviour of the drift analysis program was edited. The maximum half-power zenith angle was set to 40 degrees. This is the threshold of the zenith angle for which sources are chosen. The zenith is measured from the vertical axis. Zenith angles higher than 40 degrees are not considered. The threshold for the calculated vertical velocity was set equal to 200 m/s. If the calculated velocity is higher than this threshold the value takes the value of the threshold. This threshold is a good approximation to reality as the vertical velocity of the ionosphere is most of the cases much lower than 200 m/sec. The threshold for the evaluated horizontal velocity was set equal to 2000 m/s. This value covers extreme cases of very high ionospheric drift velocity. The upper threshold of height for which sources are selected is 700 km, which is quite high value so that the F2 region is also included, while the lower threshold of height for which sources are selected was set equal to 90 km, is a good threshold for inclusion of the E region.

The output of a drift ionogram is stored on a DFT file. All files are controlled by inspecting the amplitude of each receiver separately, aiming at checking the reliability of each individual measurement. In Figure 9 we present the performance of the four receiving antennas during two drift soundings on February 2005 at 0852UT and on 25 February 2005 at 12:36 UT. It is obvious that in the first case the Antenna 4 was blocked and the measurement cannot be used for the drift data analysis. In the second case the problem is recovered.

Channel 4 Error (2005 Feb 16 08:51:57)

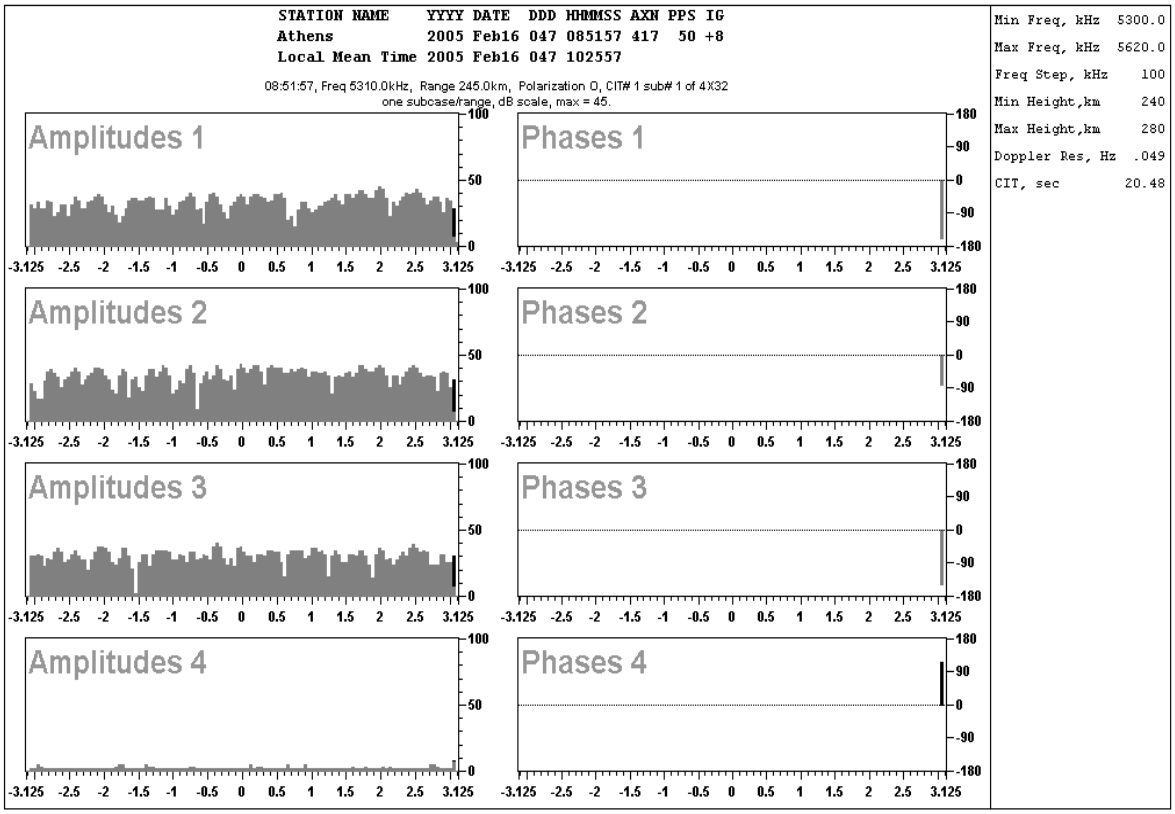

Channel 4 Repaired (2005 Mar 25 12:36:57)

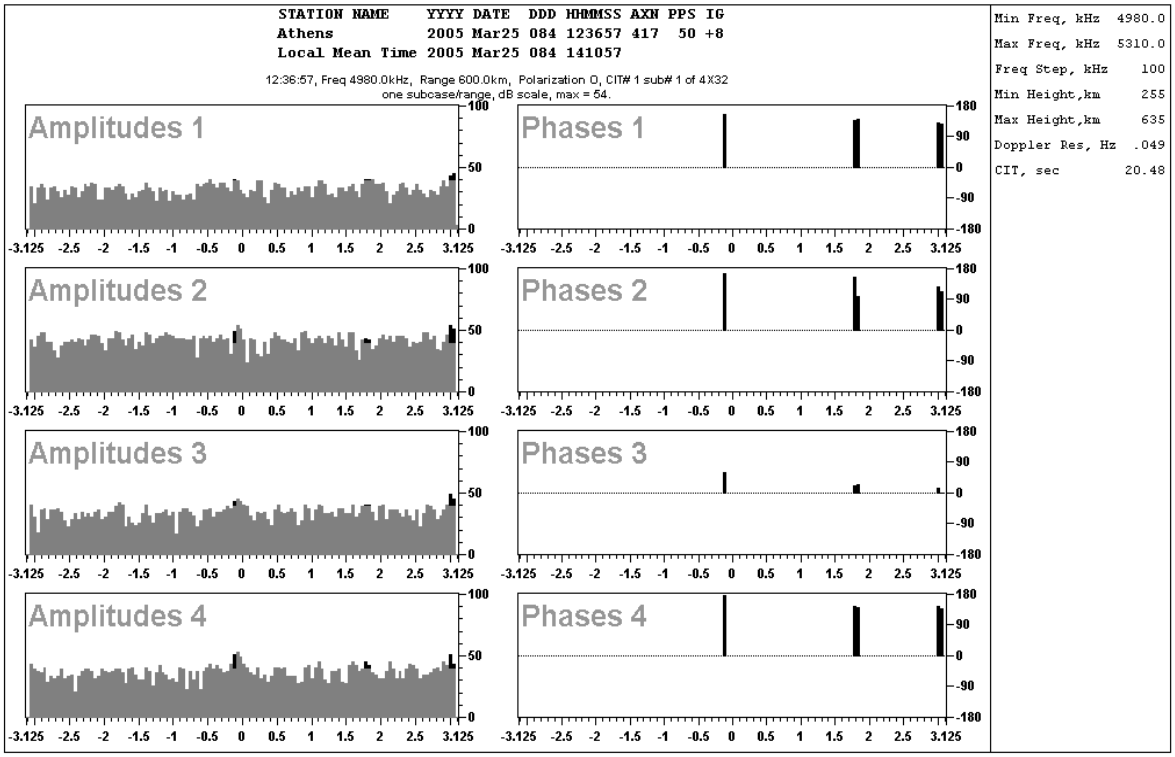

Figure 9: The performance of the four receiving antennas during for two different soundings.

Until August 2004, the DPS-4 system was performing a single drift sounding in autodrift mode. This means that the starting frequency of the sounding was automatically selected from the preceding ionogram. Thus the resulting drift velocities evaluated were those in the F layer. In order to perform research separately for the F and E region, it was decided that a different schedule should be implemented with two different soundings succeeding each ionogram. The first sounding is for the F region so the frequency is selected automatically, as before. The second sounding must have a fixed starting frequency. From experience the frequency at which significant phenomena appear in the ionogram in the E region is around 4 MHz.

In Figure 10 we present an RSF ionogram with the two subsequent sky maps for the F and E region created separately.

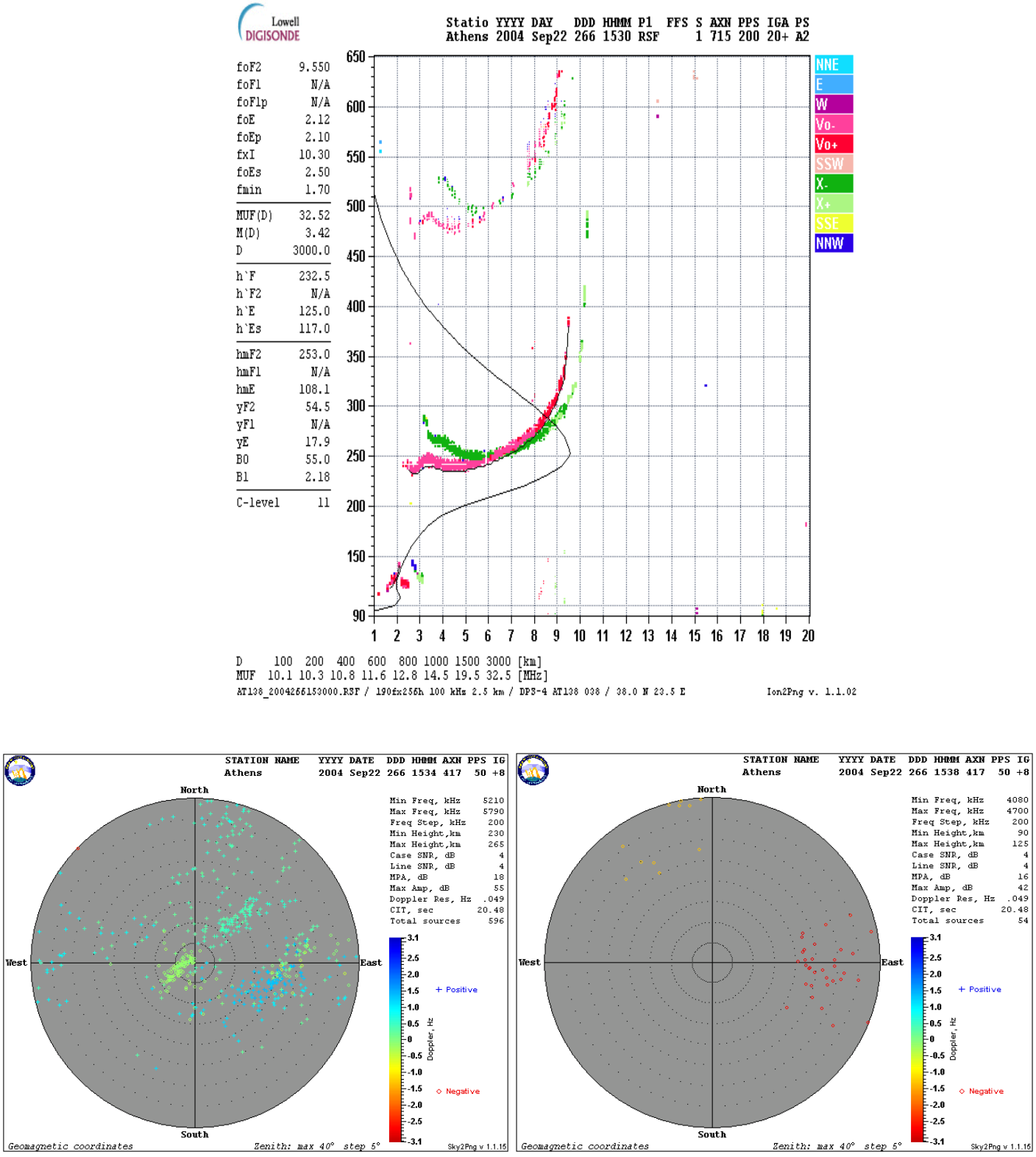

Figure 10: An RSF ionogram with the two subsequent sky maps for the E and F region.

3. Assessment of HF drift data reliability based on Athens Digisonde observations

Having collected – and checked for their reliability – observations from three equinox months, the next step is the identification of patterns and regular structures in the motion of the overhead ionosphere. The work done was organized in two steps. First, an attempt was made to determine quiet magnetospheric conditions according to the AE index. The corresponding ionospheric drift measurements obtained from Athens Digisonde at F layer heights during these intervals were statistically treated in order to extract the quiet daily drift pattern. As a second step, the effect of substorms to the quiet time drift pattern was also investigated during days characterized by high auroral activity.

3.1 Derivation of the quiet-time ionospheric drift pattern for Athens site

Aiming at the derivation of the quiet-time ionospheric drift pattern over Athens, ionospheric drift measurements obtained from Athens digisonde during quiet conditions were analysed. Six quiet days during September and October 2004 were identified, in order to investigate the pattern during equinox time. The selection was based on the daily plots of AE index (http://swdcwww.kugi.kyoto-u.ac.jp/aedir/index.html).

The selected quiet days are:

30 September 2004
17 October 2004
18 October 2004
23 October 2004
26 October 2004
28 October 2004

The quiet pattern was extracted based on observations taken during these days and therefore the results are valid for the state of the ionosphere over Athens in equinox months. The daily plots of the three velocity components Vnorth (Vn), Veast (Ve), and Vz are given in Figure 11. For each vector component the averaged value is plotted together with the standard deviation.

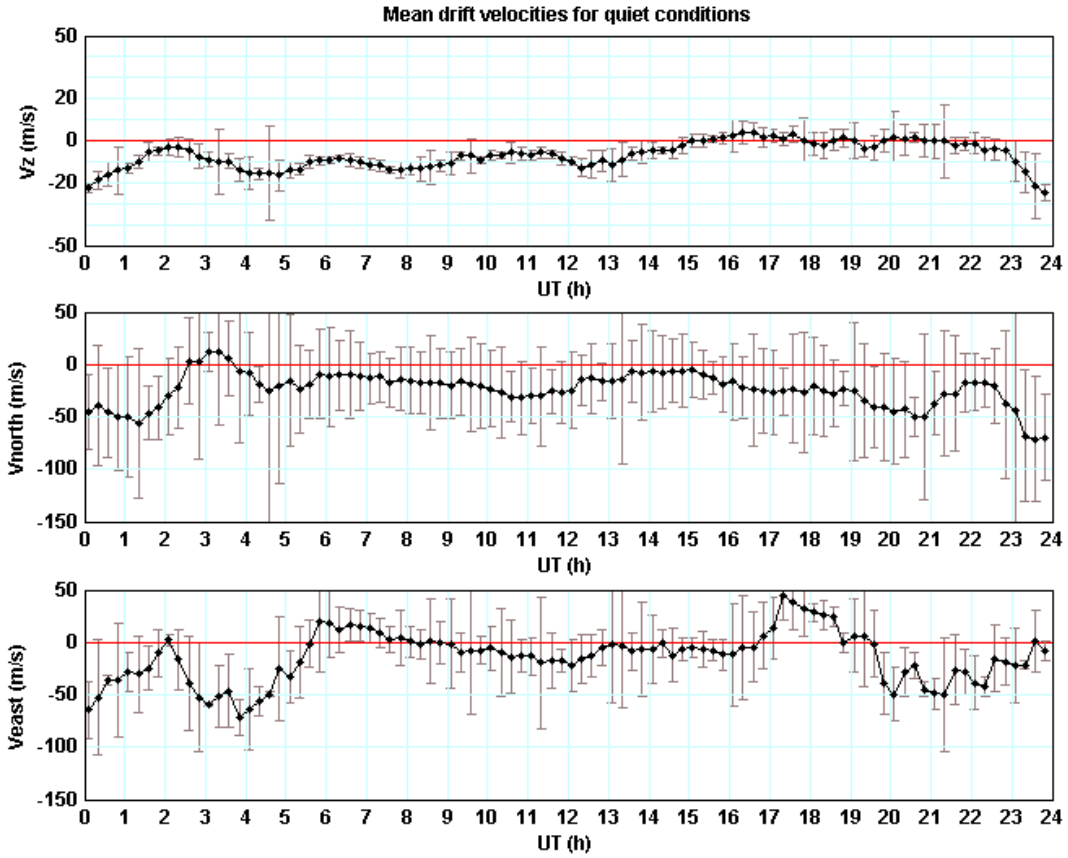

Figure 11: The daily pattern of drift velocities during quiet conditions in the equinox over Athens.

As a coarse observation, one can argue that in quiet conditions the Ve component varies with a period higher than semi-diurnal, with higher amplitude in the evening and early morning hours. The east-west drifts tend to have a daily mean westward component presenting drastic eastward increase in the sunrise and sunset. The northward (Vn) component during quiet conditions varies also with a period higher than semi-diurnal. This component presents its largest amplitude during nighttime hours and it is mainly southward oriented. The vertical component (Vz) tends to present a daily pattern with a periodicity higher than semidiurnal, but the picture is not clear enough. In general this component presents the smallest amplitude which roughly exceeds the 20m/s. This is what is expected during quiet conditions since Vz is mostly affected by atmospheric disturbances while the electromagnetic drifts affect mostly the horizontal velocity. To analyse further the motion in the horizontal plane during quiet conditions we present in Figure 12 the variation of the northward versus the eastward component. Two are the main remarks: There is a symmetrical motion of the horizontal velocity vector in respect to the east-west axis. The motion is mainly directed southward.

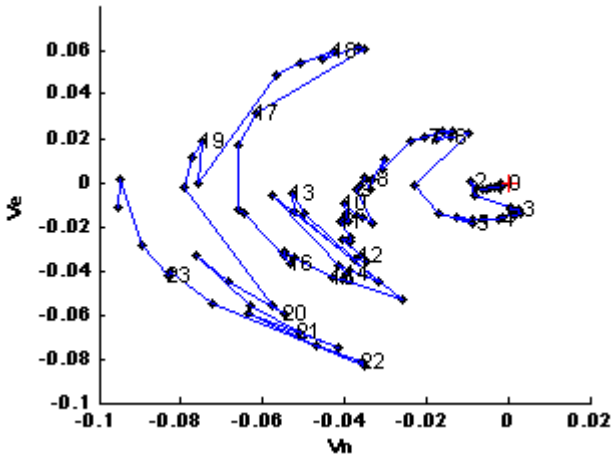

Figure 12: Ionospheric motions in the horizontal plane during quiet conditions observed in the equinox months over Athens.

3.2 HF Drift observations during substorms

The effect of magnetospheric substorms to the quiet daily pattern of ionospheric motions observed over Athens is investigated by examining two characteristic cases where auroral activity caused TAD effect over Athens. In Figure 13 we present the observations for the two selected days, 14 September 2004 and 25 October 2004. The blue lines correspond to the monthly median values for the case of foF2 and hmF2 while for the case of the drift velocity components, the blue lines correspond to the quiet pattern shown in Figure 15.
During both days the substorm activity caused uplifting of the F2 layer clearly seen in the hmF2 plot and significant daytime positive effect of short duration. All velocity components exhibit a strong disturbance in comparison to the quiet pattern, especially during nighttime hours. During the daytime, there is an increase of the vertical component that follows the variation of the true height hmF2. This provides us with a strong indication of clear TAD effect in the vertical drift component.
In addition the motion in the horizontal plane presented in Figure 14 is considerably altered comparing to the quiet conditions presented in Figure 12. There is a significant disturbance in the east-west direction especially during the second day, probably due to electric fields effect. In the north-south direction one could observe the secondary effect of TADs moving ions along the magnetic field lines.

3.3 The auroral activity effect in HF drift measurements

The main contributor in F-region ionospheric drift motions is the ionospheric electric field. This field at middle and low latitudes on magnetically quiet conditions is believed to be produced mainly by the dynamo action of thermospheric winds (e.g., Richmond, 1979), and causes the ionospheric and plasmaspheric plasmas to drift perpendicular to the geomagnetic field

(Richmond, 1976). Richmond et al., (1980) in an empirical study used seasonally averaged quiet-day (Kp<3) F-region ionospheric ExB drift observations (horizontal drift vector components) from the Millstone Hill, St. Santin, Arecibo and Jicamarca incoherent scatter radars to produce a model of the middle and low latitude electric field for solar minimum conditions. This model was designed to serve as a reference standard of electrodynamic drifts over middle and low latitude ionosphere for studies requiring this information. These model drifts could be compared to these from Athens (38.1°; 36.2°) digisonde, as a first test of the reliability of Athens digisonde drift measurements.

According to Richmond et al., (1980) model drifts for equinox time and middle-to-low latitudes, the upward/poleward drift tends to a semidiurnal behavior but with small amplitudes. This result is quite reasonable since it is fairly well established that the semidiurnal atmospheric tide dominates in the mid-latitude region (Chapman and Lindzen, 1970). Thus the results are fairly consistent with a tidal E-region source, in particular for the daytime zonal electric field (meridional drift component).

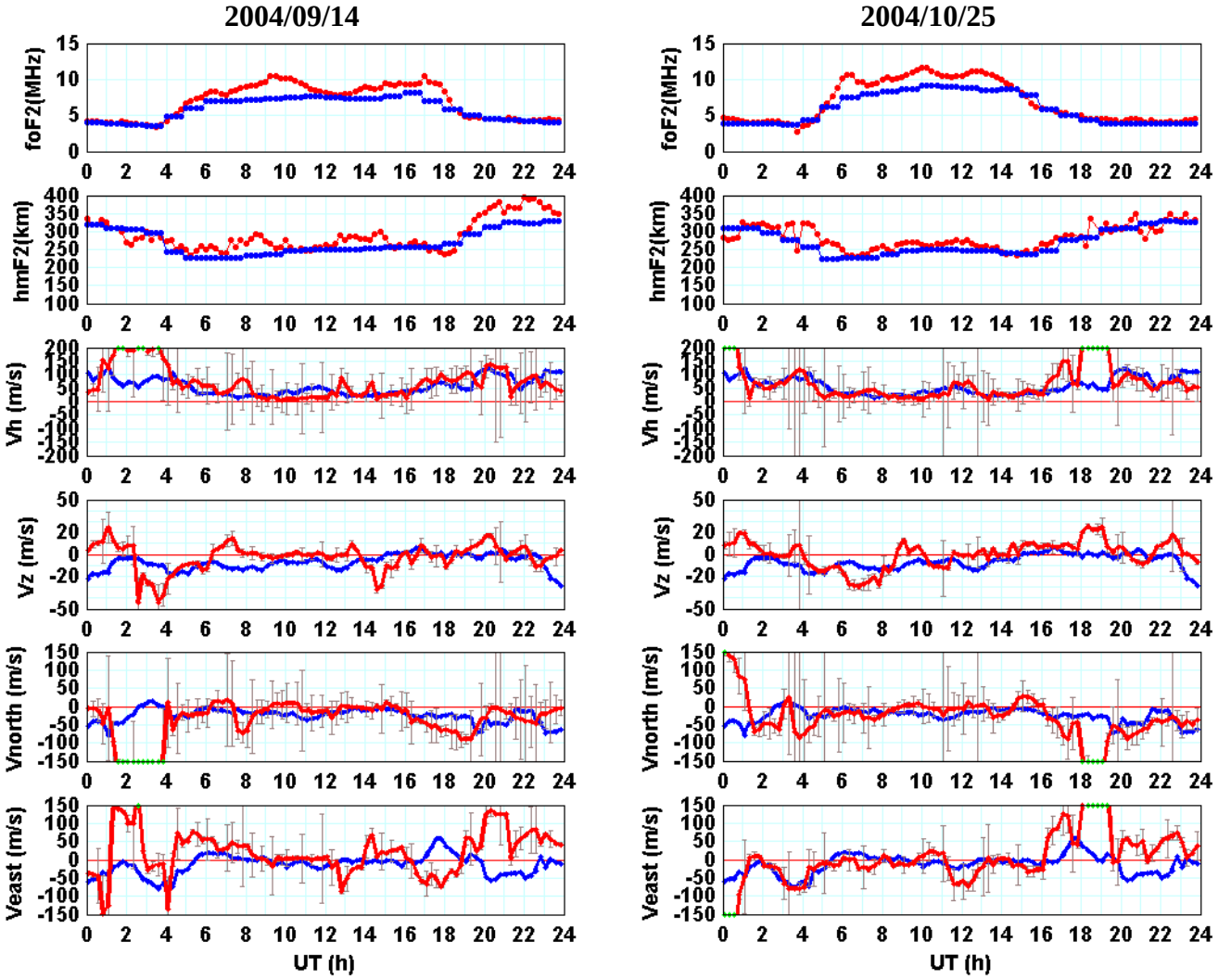

Figure 13: The variation of the foF2 and hmF2 ionospheric parameters and of the three components of the drift velocities for two disturbed days.

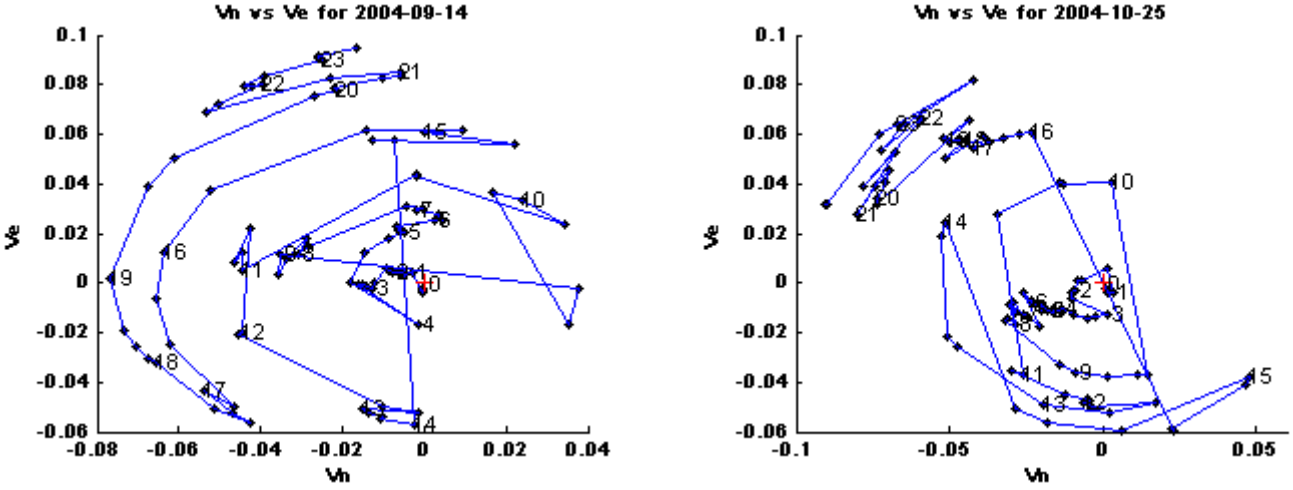

Figure 14: Ionospheric motions in the horizontal plane for two days with intense substorm activity

The meridional electric field component (zonal drift component) seems dominated by a diurnal variation. The east-west drifts tend to have a daily mean westward component at higher latitudes and a daily mean eastward component at low latitudes. It seems curious that one component exhibits a semidiurnal modulation and the other a diurnal one. It may be that two dynamos (E- and F- region) conspire to yield a diurnal pattern for the meridional electric field (zonal drift) at middle latitudes (Kelley, 1989).

The first step of this work was the derivation of the quiet daily drift velocity pattern established on Athens Digisonde observations. Several quiet days were selected based on the auroral activity as it expressed by the AE index and the behaviour of each of the three velocity components (Ve, Vn, Vz) was considered independently, during equinox months. According to our analysis, a clear enough daily pattern was identified for the Ve and Vn components which is in general agreement with Richmond et al., (1980) model drift pattern. On the other hand, the Vz component tends to present a daily pattern with a periodicity higher than semidiurnal, but the picture is not clear enough. Moreover, it appears to vary significantly during the early morning and the late evening hours and Vz's general pattern is significantly distorted during disturbed conditions.

The above findings are consistent with the argument that the electric field effects are better recognized in the Ve-Vn plane and as a result the horizontal drift velocity component is simpler to be analyzed. On contrary, the vertical component, which absorbs ionization motions due to a large number of factors, such as gravity gradients, neutral winds, ion pressure gradients and

travelling ionospheric disturbances, appears to have a rather random behavior. Indeed, during periods of enhanced auroral activity, this component seems to be the most disturbed one.
The above results give preliminary evidence that the Athens Digisonde drift observations may be used in the monitoring of the ionospheric drift motions. Moreover, the analysis of drift observations could lead to significant results concerning the deeper understanding of the ionospheric electrodynamics.

4. Development of new web tools for the best exploitation of the ionospheric drift observations

4.1 Development of a web tool demonstrating the daily plots of the E and F region drift velocities updated in real-time

For the real time calculation of the E and F region drift velocities, a MATLAB code was developed and installed in the web server of Athens Digisonde (www.iono.noa.gr). The program activates 5 minutes after each sounding. The functional diagram, to give a rough outline of the structure of the application is given in Figure 15.

Figure 15

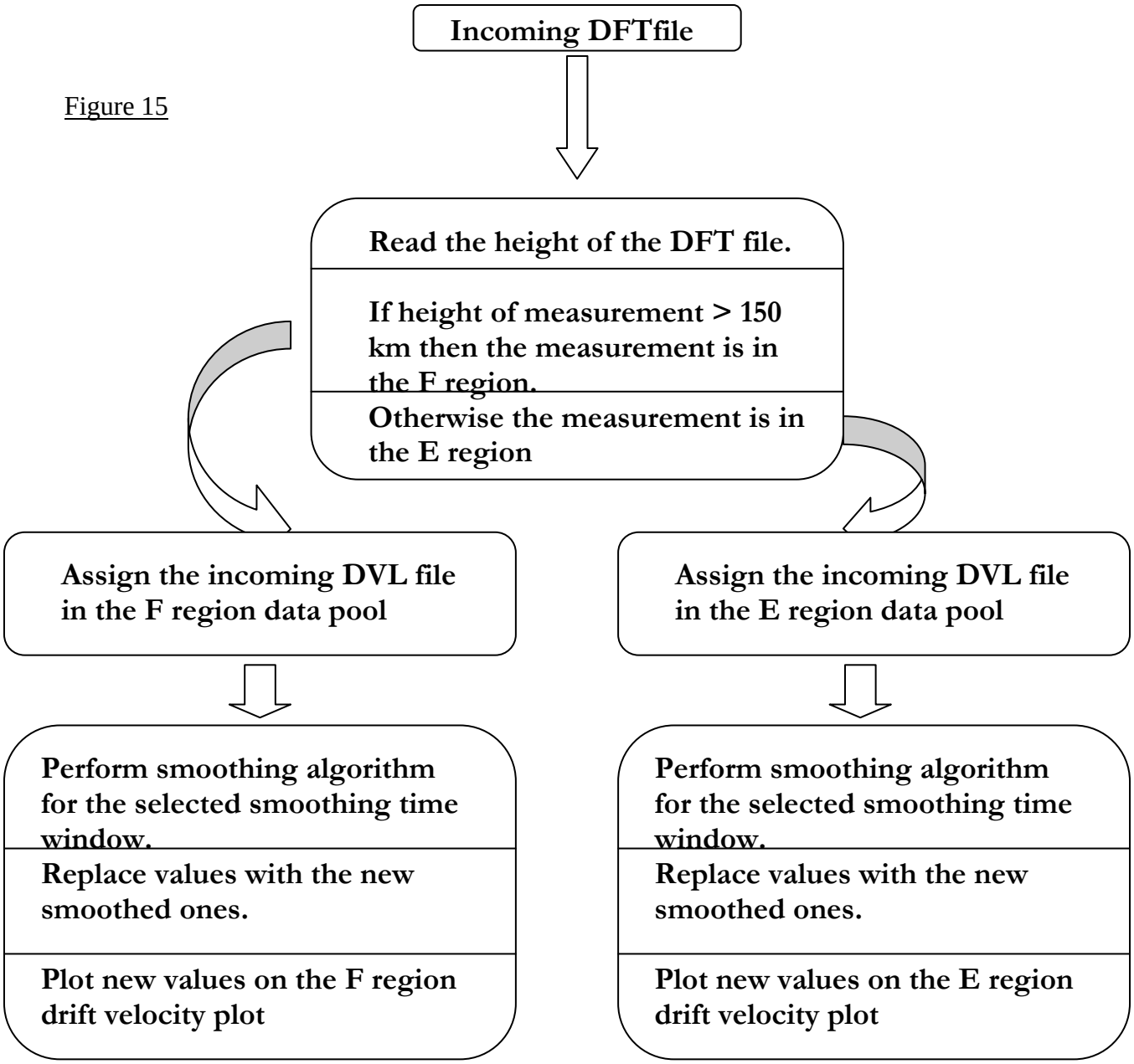

The smoothing operation seen in the above block diagram is performed in order to eliminate occasions of very rapid consequent changes, which tend to happen due to errors. The smoothing algorithm is using a time window with length chosen by the user. The length of the smoothing window has been chosen to be 90 minutes. This window spans ±45 minutes from the center of the window, which is considered the current measurement. As each measurement for the F or the E regions is taken every 15 minutes, this is translated into 5 measurements falling into the smoothing windows, the middle one been the current measurement. Every time a new measurement is taken, the smoothing window is set with each end at the new measurement and slides until the new measurement reaches the middle of the window. This means that the last 3 measurements, including the new one, are changed every time the smoothing operation is performed. These 3 changed values are placed into the drift velocity graph after the smoothing algorithm stops.
The following Figures 16 and 17 present the two separate daily plots of the E and F region drifts as appeared on the web (http://www.iono.noa.gr).

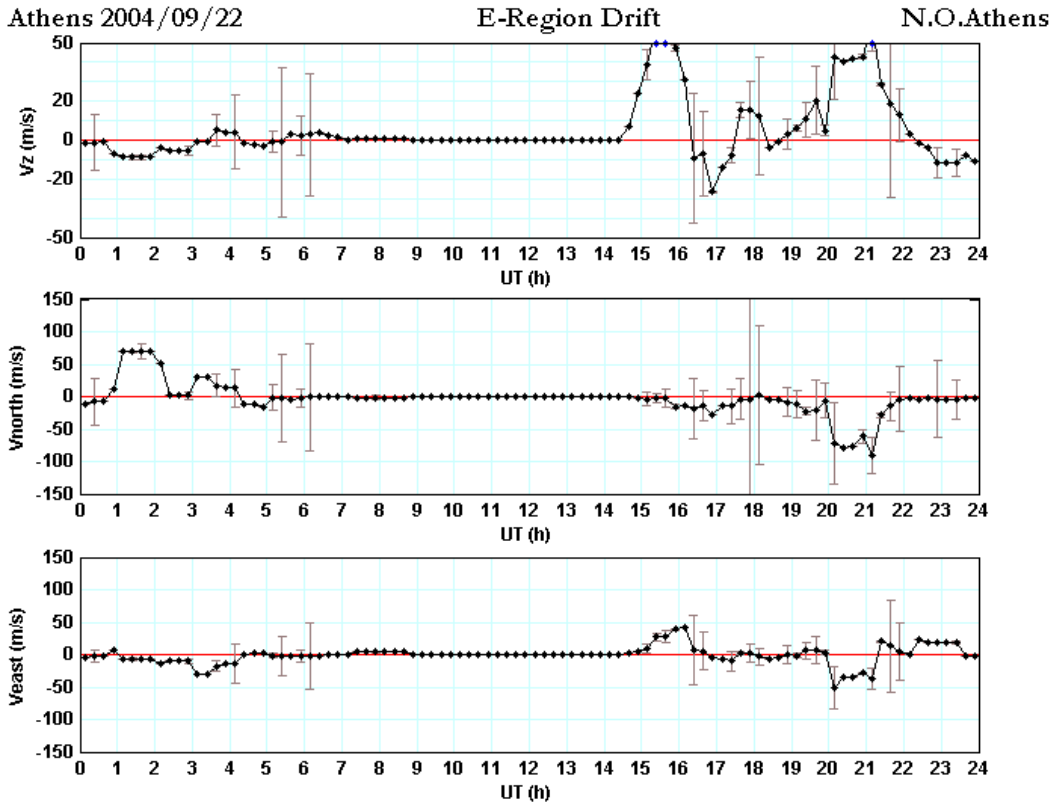

Figure 16: Daily plot of the E region drift velocities measured using Athens Digisonde observations

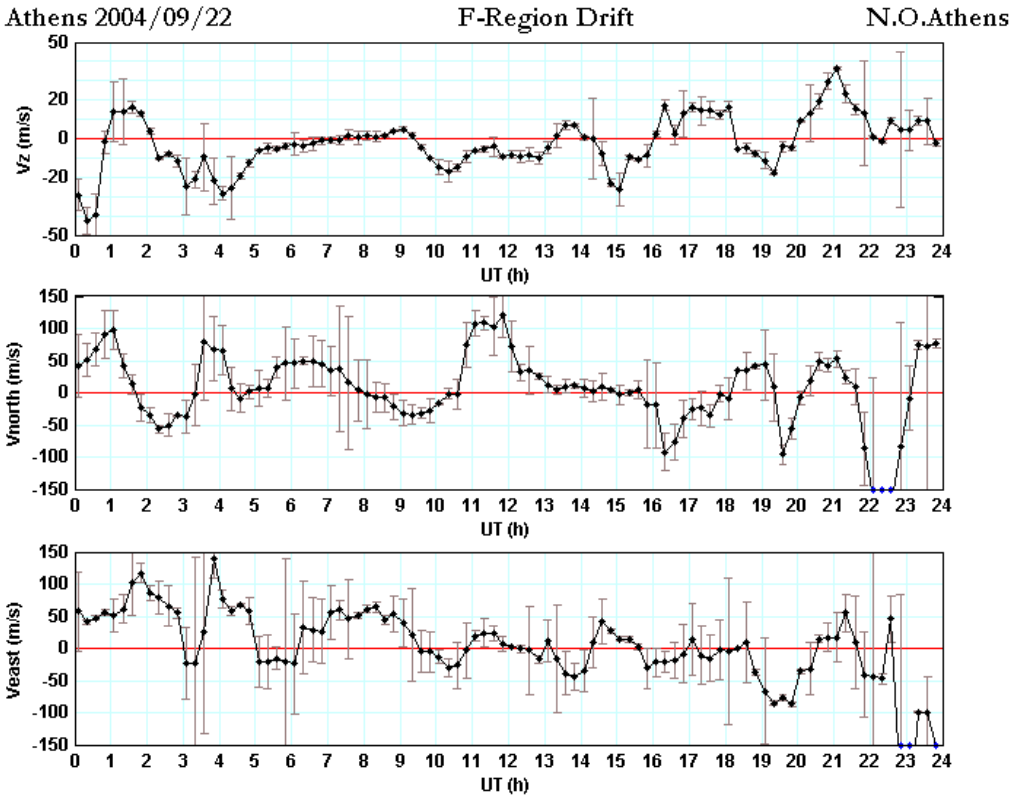

Figure 17: Daily plot of the F region drift velocities measured using Athens Digisonde observations

Historical drift measurements are available on the archive that is kept on the Athens Digisonde web site (Figure 18).
The access to all drift measurements in real-time and archived format is provided for free to all subscribed users.

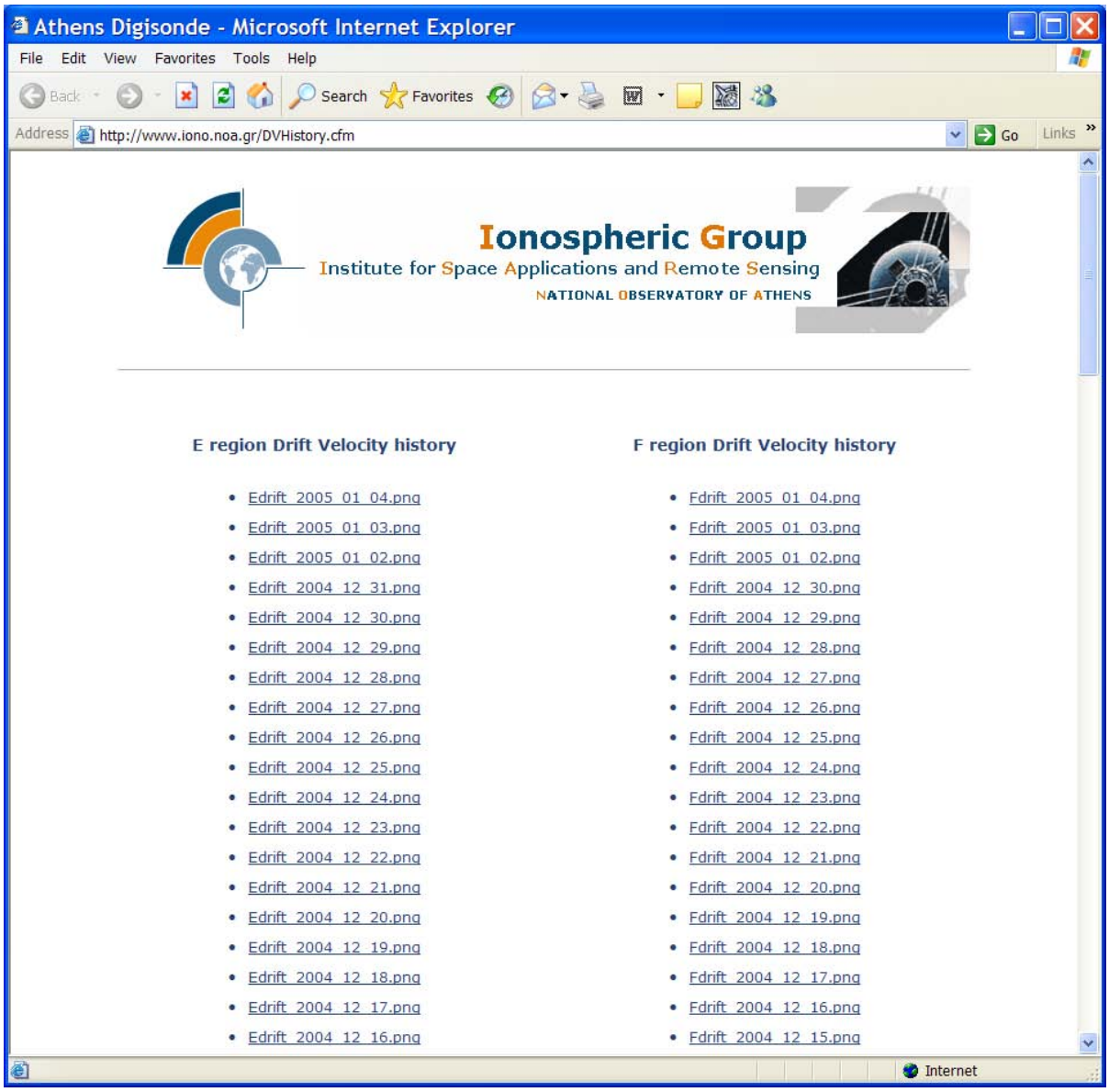

Figure 18: Historical drift measurements in Athens Digisonde web site

4.2 Development of a web tool for the assessment of the reliability of Athens Digisonde drift observations

As it is already mentioned, in case of HF radars such as the Digisonde, where motion is deduced from a measure of Doppler shifts on radiowaves reflected from the ionosphere a further distinction needs to be made. The Digisondes measures the Apparent Velocity “Va”, which is a complicated function of a number of time varying properties of the radio wave propagation medium. For instance the Doppler frequency shift is affected by both the motion of the reflecting surface and the time variation of the refractive index along the ray. In the ionosphere the time changes in the refractive index arise from the ionospheric motions and also from production and

loss of ionization. When interpreting velocity measurements obtained from the Digisonde Drift Analysis method, care must be taken in relating the motion to the effects of photoionization, recombination, gravity waves and plasma motion.

In particular, the effect of gravity waves in the midlatitude ionosphere is summarized in the generation of atmospheric disturbances at auroral latitudes and their propagation toward the equator. These disturbances alter the ionospheric characteristics and are known as Traveling Atmospheric Distubances (TADs). The most well recognized signature of the TADs is the increase in the true height of the F2 layer, accompanied by and increase in the ionospheric ionization and of course in foF2. Moreover, the effect of the TADs on the drift observations is discussed in detail in Section 3. Therefore, in order to provide the user with all necessary information concerning the interpretation of the drift observations, a new website was developed, providing the ionospheric conditions in the F region (expressed by foF2 and hmF2) determined by the vertical scanning and the calculated drift velocities determined by the autodrift measurement (http://www.iono.noa.gr/quietdrift.cfm). This web site is a useful tool for visual inspection (quick look) of the ionospheric conditions during a particular day and of the measured velocities of ionospheric motions determined over Athens. It is expected that during very quiet conditions the measured velocities are due to ExB drifts solely.

In Figures 19 and 20, the homepage of this website and an example of the provided information are given.

Figure 19: This page (http://www.iono.noa.gr/quietdrift.cfm) provides access to daily plots of the foF2 and hmF2 ionospheric characteristics together with the ionospheric drift velocity components [Vh, Vz, Vn, Ve], obtained by the Athens Digisonde during equinox months.

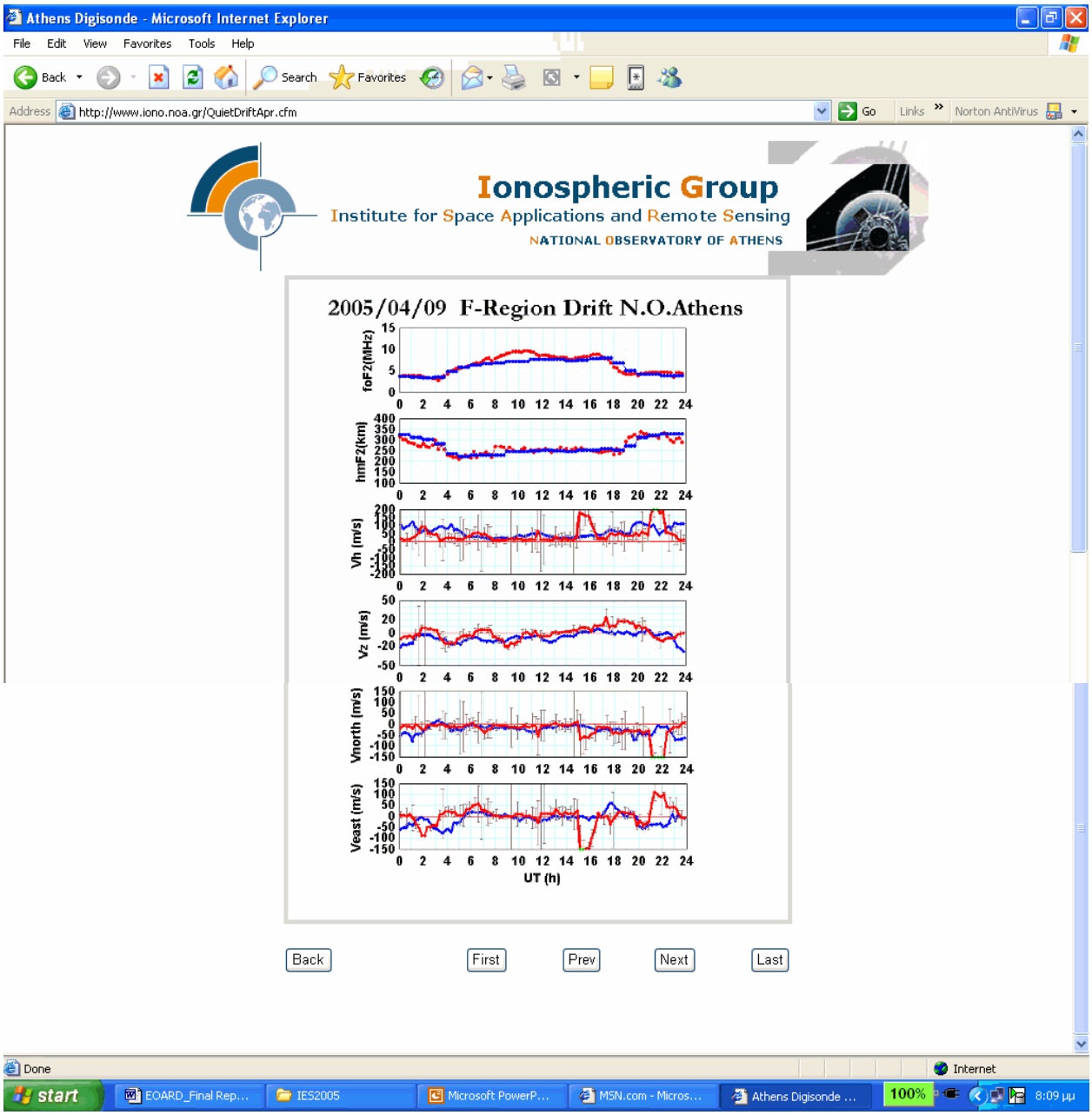

Figure 20: Example showing the quick look of the F-layer conditions and the calculated drift velocities on 9 April 2005. The red lines in the plots correspond to actual measurements, while the blue ones correspond to monthly median values in the case of foF2 and hmF2 and to the quiet-time drift pattern in the case of the drift velocity components.

Summary

The work done in the frames of this project was organized in two steps. First, an attempt was made to determine quiet magnetospheric conditions according to the AE index. The corresponding ionospheric drift measurements obtained from Athens Digisonde at F layer heights during these intervals were statistically treated in order to extract the quiet daily drift pattern. The preliminary comparison of the derived ionospheric drift pattern with previously reported results extracted from the analysis of observations from middle latitude ISR stations gave evidence for reliable ionopheric drift measurements with Athens digisonde. Moreover, suggestive conclusions about the mechanisms contributing to the quiet ionospheric drift pattern over Athens are obtained. As a second step, the effect of substorms to the quiet time drift pattern was also investigated during days characterized by high auroral activity. The quiet drift pattern appears distorted during these days, providing additional evidence about the predominance of ExB drifts in Athens Digisonde observations during quiet periods. The findings are valid for the fall months.

Further investigation is required in order to establish more reliable results, aiming to their application for scientific or operational purposes. Therefore the daily quiet pattern for each season of the year will be calculated as more data will be stored in our database. It will be then possible to compare the extracted pattern with the output of the model by Richmond et al. (1980) that is designed to serve as a reference standard of electromagnetic drifts over middle and low latitude ionosphere.

Finally it is our future goal to apply this methodology to the E region aiming at further studies of sporadic E layers.

References

Bennett J.A., Aust. J. Phys., 21:259, 1968.

Bibl, K. and Reinisch, B. W., The universal digital ionosonde, Radio Sci., 13, 519-530, 1978.

Blanc E. and Hougninou E., Typical disturbances of the daytime equatorial F-region observed with a high resolution HF radar, Ann. Geophysicae, 16:721–730, 1998.

Briggs B.H., Phillips G.J., and Shinn D.E., The analysis of observations on spaced receivers of the fadings of radio signals, Proc.Phys.Soc.London, 63(B): 106–121, 1950.

Brownlie G.D., Dryburgh L.G., and Whitehead J.D., Measurement of the velocity of waves in the inoosphere: A comparison of the ray theory approach and diffraction theory, J.Atm.Terr.Phys., 35:2147–2162, 1973.

Cannon P.S., Reinisch B.W., Buchau J., and Bullett T.W., Response of the polar cap f region convection direction to changes in the interplanetary magnetic field: digisonde measurements in northern Greenland, J.Geophys.Res., 96(A2):1239–1250, 1991.

Chapman, S. and Lindzen, R.S., “Atmospheric Tides: Thermal and Gravitational”, Gordon and Breach, New York, 1970.

Dyson P.L., Relationships between the rate of change of phase path (Doppler shift) and angle of arrival, J.Atm.Terr.Phys., 37:1151–1154, 1975.

From W.R., Sadler E.M, and Whitehead J.D., Measuring ionospheric movements using totally reflected radio waves, J.Atm.Terr.Phys., 50(2):153–165, 1988.

Georges T.M., HF Doppler studies of Travelling Ionospheric Disturbances, J.Atm.Terr.Phys., 30:735–746, 1968.

Harnischmacher E. and Rawer K., Drift observations evaluated by the method of similar fades, J.Atm.Terr.Phys., 13:1–16, 1958.

Herron T.J. and Donn W.L., Diurnal variations of F-region waves, J.Atm.Terr.Phys., 35:2163–2176, 1973.

Hines C.O., Can.J.Phys., 38:1441, 1960.

Jacobi C., Schminder R., and Krschner D., Measurements of mesopause region winds over central Europe from 1983 through 1995 at collm, Germany, Beitr. Phys.Atmosph., pages 189–200, 1997.

Jacobi C., Schminder R., and Krschner D., Planetary wave activiy obtained from long-period (2-18 days) variations of mesopause region winds over central Europe (52on, 15eo), J.Atm.Terr.Phys., 60(1):81–83, 1998.

Kelley, M.C., “The Earth’s Ionosphere”, Academic Press, San Diego, California, 1989.

Krautkrmer J., Windmessungen in der ionosphre, Arch. Elektr. Bertragungen, 4:133–141, 1950.

Mitra S.N., A radio method of measuring winds in the ionosphere, Proc. Inst. Electr. Eng., 3(96): 441–446, 1949.

Munro G.H., Travelling ionospheric disturbances in the F-region, Aust.J.Phys., 11:91–112, 1958.

Parkinson M.L., Monselesan D.P., Smith P.R., Dyson P.L., and Morris R.J., Digital ionosonde measurements of the height variation of drift in the southern polar cap, J. of Geophys. Res., 102:24075–24090, 1997.

Parkinson M.L. and Dyson P.L., Measurement of mid-lattitude E-region, sporadic-E and TID related drifts using HF doppler-sorted interferometry, J.Atm.Terr.Phys., 60(5):509–522, 1998.

Pfister W., The wave-like nature of inhomogeneities in the E-region, J.Atm.Terr.Phys., 33:999–1025, 1971.

Pfister W., Drift measurements with spectral analysis during periods of chemical releases into the ionosphere, Methods of measurements and results of lower ionosphere structure. Akademie Verlang, Berlin, 1974.

Phillips G.J. and Spencer M., The effects of anisometric amplitude patterns in the measurements of ionospheric drifts, Proc.Phys.Soc.London, 68(B):481–492, 1955.

Rawer K., Wave propagation in the ionosphere, Kluwer Academic Publishers, 1993.

Reinisch B.W., Buchau J., and Weber E.J., Digital ionosonde observations of the polar cap F region convection, Phys. Scr., 36:372–377, 1987.

Reinisch B.W., Modern Ionosondes in Modern Ionospheric Science, Eds. Kohl, H., Rüster, R., and Schlegel, K., European Geophysical Society, 37191 Katlenburg-Lindau, Germany, 440-458, 1996.

Reinisch Bodo W., Scali James L., and Haines D. Mark, Ionospheric drift measurements with ionosondes, Annali di Geofisica, 41(5-6):695–702, 1998.

Richmond A.D., M. Blanc, B.A. Emery, R.H. Wand, B.G. Fejer, R.F. Woodman, S. Ganguly, P. Amayenc, R.A. Behnke, C. Calderon, and J.V. Evans, An empirical model of quiet-day

ionospheric electric fields at middle and low latitudes, J. Geophys. Res. 85, A9, 4658-4664, 1980.

Richmond, A.D., Electric fields in the ionosphere and plasmasphere on quiet days, . Geophys. Res., 81, 1447-1450, 1976

Richmond, A.D., Ionospheric wind dynamo theory: A review, J. Geomagn. Geoelec. 31, 287-310, 1979.

Scali J.L., Reinisch B.W., Heinselman C.J., and Bullett T.W., Coordinate digisonde and incoherent scatter radar F − region drift measurements at sondre stromfjord, Radio Science, 30(5):1481–1498, 1995.

Scali J. L., Digisonde drift analysis, Technical report, Center for Atmospheric Research, University of Massachusetts at Lowell, http://umlcar.uml.edu, July 1993.

Smith P.R., Dyson P.L., Monselesan D.P., and Morris R.J., Ionospheric convection at Casey, a southern polar cap station, J.Geophys.Res., 103(A2):2209–2218, 1998.

Spenger K. and Schminder R., Results of 10 years' ionospheric measurements in the LF range, J.Atm.Terr.Phys., 29:183–199, 1967.

Toman K., J.Geophys.Res., 60:57, 1955.

Whitehead J.D. and Monro P.E., Phase and amplitude analysis of radio echoes from the ionosphere, J.Atm.Terr.Phys., 37:1427–1430, 1975.

Wilson M.J., Pfister's space characterisation of ionospheric movements, J.Atm.Terr.Phys., 57(14):1733– 1752, 1995.